Synthesis and Characterization of Organic Radical Polymers

A Thesis

Presented to the Faculty of the Graduate School

of Cornell University

In Partial Fulfillment of the Requirements for the Degree of

Master of Science

By

Fan Fan

August 2016

© 2016 Fan Fan

ABSTRACT

Organic radical polymer batteries have emerged as promising alternatives to conventional Li-ion batteries, for their mechanical flexibility, extraordinary cyclability, high power, and fast charge transfer kinetics.

This research focuses on the design and synthesis of diblock copolymers, which incorporate an intrinsically conductive conjugated block of poly(3-hexylthiophene) (P3HT) through Grignard metathesis polymerization and organic radical functional groups included in a block as poly(2,2,6,6-tetramethylpiperidinyloxy-4-yl methacrylate) (PTMA) through atom transfer radical polymerization (ATRP). Different molar ratios of P3HT and PTMA were achieved and further verified by GPC, NMR and UV-vis absorption, while the improved quenching method could better control molecular weight dispersity. The AFM images showed different tendencies from stripe-like to hole-like microstructures of P3HT-b-PTMA based on different thin film preparation methods. The resistance of P3HT thin films was obtained and device models were proposed to study the resistance parameters of P3HT-b-PTMA.

BIOGRAPHICAL SKETCH

Fan Fan was born in Sichuan, China on July 14 1992. Quite interested in chemistry and physics classes in the high school, she decided to major in materials science and engineering at Tianjin University in 2010. She was encouraged to do lab research by Prof. Wei Feng, and did lab work focusing on electrochemical properties of polyaniline from 2012 to 2013. In 2014 spring, she was selected by Prof. Alex O. Anning in Materials Science and Engineering of Virginia Tech (VT) to carry out her senior year graduate project, which was funded by China Scholarship Council (CSC). The project concentrated on mechanical alloying, and she worked more with high-energy milling and compression modeling. Inspired by the undergrads research experience, she pursued her master degree in Cornell University in the fall of 2014. Planning to step further in the polymer pathway, she chose to join Prof. Ober's group, and mainly worked on fundamental studies of stable radical polymers for energy storage. She hopes to continue working in the polymer field upon completion of the degree.

ACKNOWLEDGMENTS

I would like to first thank my advisor, Prof. Christopher K. Ober, for his guidance. I also thank my committee members, Prof. Emmanuel P. Giannelis for allowing the usage of his facilities.

I would thank Prof. Greg Fuchs for the collaboration with our project, and his valuable suggestion and discussions.

I would thank Dr. Clemens Liedel, who introduced me to my graduate project, trained me various techniques and assisted me through research problems.

I would thank the staff at CNF, CCMR, and CU-KAUST, for their assistance and guidance in running instruments and data processing.

I would thank my department colleagues and staff for their help.

I would specially thank my parents, for their support during my Master of Science study.

TABLE OF CONTENTS

LIST OF FIGURES

LIST OF TABLES

Chapter 1 Introduction

Block copolymers are a special group of polymers that are composed of two or more covalently attached homopolymer building blocks. It is becoming a promising material for its ease to self-assemble into different nanostructures [1]. Conjugated polymers are attracting more attention as alternatives to traditional inorganic semiconductors for their solution processability and thus device flexibility. They possess the excellent electronic properties of semiconductors, and at the same time the outstanding mechanical advantages of plastics [2]. Stable radical polymers are coming into focus for their unique structure with the unpaired electron, and they are expected to have special electronic, magnetic and optical properties [3][4][5]. In order to study the fundamental mechanisms of stable radical polymers applied in energy storage, we have designed a diblock copolymer with a conjugated polymer block with a stable radical polymer block, where the conjugated polymer block, as well as the desired microphase separation, provides a better pathway for electron transportation.

In Chapter 1, we will describe a conjugated polymer, stable radical polymer and block copolymer, how they have developed to date and their character and properties. We will also present the reasons why we selected poly(3-hexylthiophene) (P3HT) as the conjugated block, as well as why the poly(2,2,2,6,6-tetramethyl-4-piperidinyloxymethacrylate) (PTMA) is chosen as the second block. In addition, we will also explain the fundamental mechanisms in our synthesis and why we selected them.

In Chapter 2, we will describe the materials used in synthesis and sample preparations for characterization, the instruments used for evaluating polymer properties, and the general routes used for organic synthesis of block copolymers. And we summarize all the different ratios of diblock copolymer made during the entire experimental study.

In chapter 3 and chapter 4, we will demonstrate all physical characterization, the microstructure characterization, and related electrical properties of our P3HT conjugated homopolymer and the P3HT-*b*-PTMA diblock copolymer. And then compare and discuss in the context of other research groups who are doing the relevant projects, to talk about their advantages and disadvantages.

1.1 Conjugated polymers

Π-conjugated polymers contain continuous paths of carbon atoms carrying a π atomic orbital. In 1976, scientists discovered that conjugated polymers could be highly electrically conducting after applying redox chemical treatment, which triggered great interest towards them [6]. In the 1980s, many research groups studied π-conjugated oligomers and polymers, to pave the way for later development of plastic electronics [7]. There was a breakthrough in 1987 by the Tang group, who made the first electroluminescent device on the basis of a π-conjugated molecular material, which helped to start the study of organic light-emitting diodes (LEDs) [8]. Conjugated polymers are attracting more attention as alternatives to traditional inorganic semiconductors for their solution processability and thus device fabrication flexibility. They possess excellent both the electronic properties of semiconductors, and the outstanding mechanical advantages of plastics [2]. In addition to these advantages, their light weight, low cost, corrosion resistance and good electronic or opto-electronic properties compared to traditional semiconductors also triggered research interest over the past decades.

The first and most common method to determine the electronic structure of conjugated systems was the one-electron Hückel technique, which was specially designed for conjugated

molecules. Later on, more detailed theoretical treatment was needed to incorporate electron correlation effects and the interchain interactions. The elaborate theory showed that electronic properties of conjugated polymers depend largely on the micromorphology of the polymer chains and the way the chains pack together in thin films, and thus could be controlled by solvent types, polymer concentration, annealing conditions, and etc. [9].

Among the entire class of conjugated polymers, polythiophene and its derivatives, especially poly(3-hexylthiophene) (P3HT) are of importance. In the field of organic electronic devices, P3HT is an important material in applications such as solar cells, LEDs [10], organic field-effect transistors (OFET) [11][12], organic photovoltaics (OPV) [13][14], etc., for its stability in the ambient environment and ease of processing in organic solution when functionalized with flexible side chains. Thus it can be fabricated into desired shapes for many useful devices mentioned above. Despite its importance in various applications in optoelectronic area, P3HT also plays a significant role in many fundamental studies, regarding understanding the transport of charges, the physics underneath the construction, and optimization of practical devices and the micromorphology of thin films [15].

1.2 Stable radical polymers

Radicals are subvalent compounds, for they have one less bond than expected based on standard considerations. Most common radicals are highly reactive which form unstable molecules and results in dimerization, hydrogen abstraction, and disproportionation to reach a thermodynamic balance [16]. In the meantime, there exists another class of radicals with properties completely different from those mentioned above. There are examples of unpaired

electron molecules which have long lifetimes. There are also examples of isolated radicals which are unreactive to air and water [17][18][19].

The stable radicals have been discovered and synthesized only a century. There exist ways to employ recyclable oligomeric TEMPO catalysts and sodium hypochlorite is used as the oxidant for the oxidation of alcohols to carbonyl compounds [20], while there exist another class of radicals which could be used as the antioxidants [21][22]. Great interest has been focused on radical-related transition metal coordination chemistry, such as the incorporation of metal-catalyzed cross-coupling and metal-templated cycloaddition reactions to produce multiporphyrin compounds [23]. Stable radicals are also involved in living radical polymerization [24] and biological synthesis [25].

There are numerous molecular structural features which may lead to the stability of radicals. Steric protection is the most universally acceptable way to provide kinetic and thermodynamic stability to a reactive radical, which incorporates bulky substituents [26]. The drawback of this approach is that, the stability of radicals depends on the spin of the stable radical to interact with other molecules chemically or magnetically. Therefore, the steric protection aiming at stability of the radicals might counteract to its original intention. Electronic distribution is another stabilizing feature, which means the probability of the spin to be delocalized over an entire π system. Delocalization is an efficient way to reduce reactivity, for the spreading of spin density over more atomic centers should dilute the amount of spin on any one atom, which in turn should decrease the reactivity of the site [16]. The disadvantage of this explanation is that, it oversimplifies “more delocalization is better”, as it ignores the differential reactivity at different atomic centers. Heteroatom-based structure is another common structure of the stable radicals, such as nitrogen, oxygen and sulfur. Because

they are “lone pair rich” which provide lone pair repulsions when two or more of these kinds of atoms are linked together, and thus result in anomalously low σ bond strengths as in peroxides or hydrazines. Therefore, this lone pair repulsion overrides any possible thermodynamic gain from the σ bond formation. Last but not least, charge distribution plays an important role in the structure for stability of radicals. However, the interaction between spin distribution and charge distribution is poorly understood [27].

Many of the most common stable radical kinds are based on nitrogen and/or oxygen, such as O_2, NO, NO_2 spin centers, among which, the nitroxides $[R_2NO]\bullet$ are the most well-known class of stable radicals. The first nitroxide has been discovered 150 years ago, named Fremy’s salt, as shown in Figure 1. 1 (a). NO-centered nitroxides with two quaternary carbon-based substituents are quite robust, such as TEMPO in Figure 1. 1 (b). Nitroxide radicals in which the NO group is conjugated to a C=N moiety, are called “imino nitroxides” (Figure 1. 1 (c)), are stable enough to be isolated. Nitronyl nitroxides received a great deal of attention for they are almost the most stable examples of nitroxides, while the R groups provide a wide variety of possibilities for processing, as shown in Figure 1. 1 (d). There are also other kinds of nitroxides, such as galvinoxyls in Figure 1. 1 (e), oxygen-centered phenoxyls in Figure 1. 1 (f), etc.

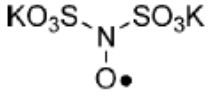

(a) Fremy’s salt

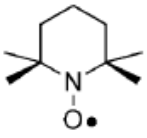

(b) TEMPO

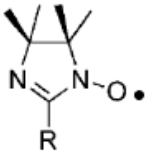

(c) Imino nitroxides

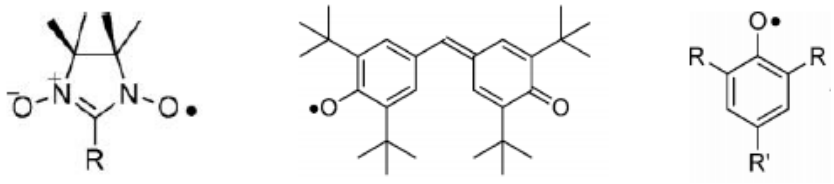

(d) nitronyl nitroxides (e) galvinoxyls (f) O-centered phenoxyls

Figure 1. 1 Examples of nitroxides structures. (a) Fremy's salt; (b) TEMPO; (c) Imino nitroxides; (d) nitronyl nitroxides; (e) galvinoxyls; (f) O-centered phenoxyls.

Polymers containing robust organic radical groups, such as NO-centered nitroxides and nitronyl nitroxides, N-centerend triarylaminium cation radicals, and O-centered phenoxyls and galvinoxyls, as pendent groups per repeating unit are an interesting class of materials [28]. Their radical redox sites allow for efficient redox gradient-driven electron transport through the polymer layer by outer-sphere self –exchange reactions in electrolyte solutions. And because of their unique structure with the unpaired electron, they could have special electronic, magnetic and optical properties [3][4][5]. The interest in nitroxides is their stability to chemical reactions carried out at remote parts of the molecules while not affecting the radical site itself [29]. And of interest in energy storage the neutral radical site(N-O•) may be reversibly altered between the radical and the oxoammonium cation (N^+=O) with stability of both redox states under ambient conditions [30].

Figure 1. 2 presents a reversible electron-transfer reaction of organic, robust, and electro-active radicals R. The oxidation ($R \bullet \leftrightarrow R^+ + e^-$) and reduction ($R \bullet + e^- \leftrightarrow R^-$) correspond to positive charging (p-type doping) and negative charging (n-type doping) of the neutral radical, respectively. This reaction is a simple one-electron transfer, where no chemical bonds are broken and no new bonds are formed. The electron transport amounts to the layer until all of the redox sites change their oxidation states [31].

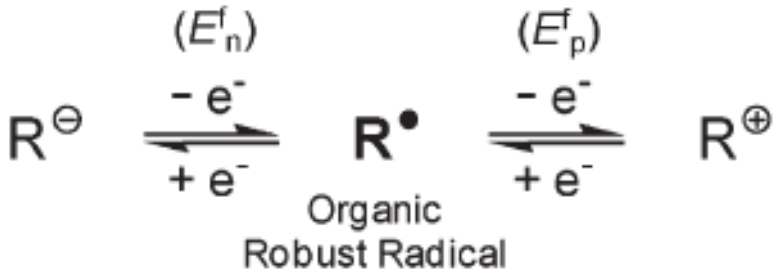

Figure 1. 2 Reversible electron-transfer reaction of radicals R• [31].

1.3 Block Copolymers

Block copolymers are a special group of polymers that are composed of two or more homopolymer building blocks linked covalently. This class of polymers a promising for its ease to self-assemble into different nanostructures with characteristic separation on a length scale of approximately 10-100 nm, to form such microstructures as lamellae, hexagonally packed cylinders, gyroids, spheres, etc., as shown in Figure 1. 3 [1].

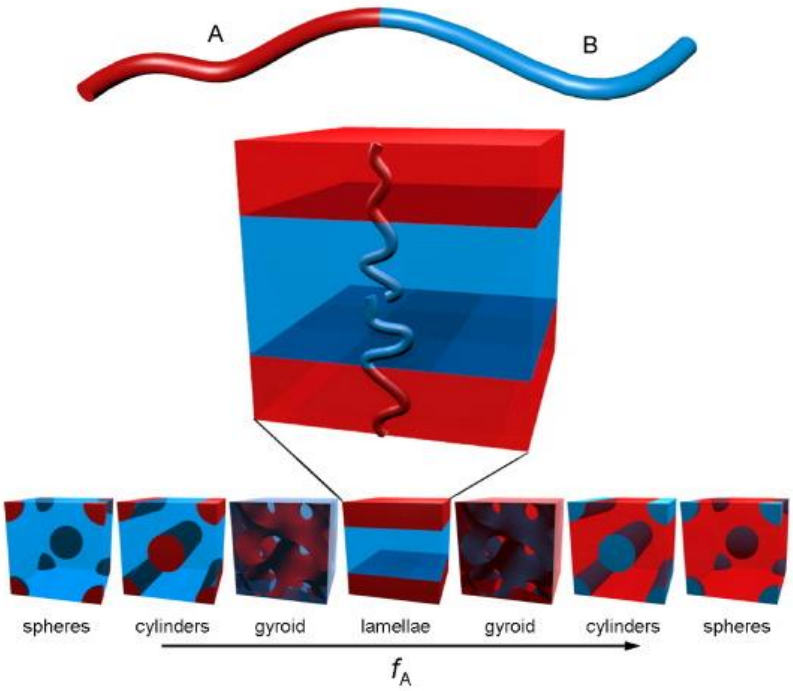

Figure 1. 3 Schematics of thermodynamically stable diblock copolymer phases. The A–B diblock copolymer represented at the top is depicted as a two-color chain for simplicity [1].

Typical coil-coil block copolymers present different kinds of phase transition due to the miscibility of the two blocks A and B, which could be expressed according to the Gibbs free energy ΔG_{mix}, as shown in $\Delta G_{mix} = K_B T \cdot \chi_{AB} \cdot \Phi_A \cdot \Phi_B + K_B T \cdot \left(\frac{\Phi_A}{N_A} \cdot ln\Phi_A + \frac{\Phi_B}{N_B} \cdot ln\Phi_B\right)$ Equation 1. 1.

$$\Delta G_{mix} = K_B T \cdot \chi_{AB} \cdot \Phi_A \cdot \Phi_B + K_B T \cdot \left(\frac{\Phi_A}{N_A} \cdot ln\Phi_A + \frac{\Phi_B}{N_B} \cdot ln\Phi_B\right) \quad \text{Equation 1. 1}$$

χ_{AB} is the Flory-Huggins interaction parameter between block A and B, which is positive for most of the polymers. Φ_A and Φ_B are volume fraction of block A and B, respectively ($\Phi_B = 1 - \Phi_A$). N_A and N_B are degree of polymerization of block A and B, respectively. The first part of $\Delta G_{mix} = K_B T \cdot \chi_{AB} \cdot \Phi_A \cdot \Phi_B + K_B T \cdot \left(\frac{\Phi_A}{N_A} \cdot ln\Phi_A + \frac{\Phi_B}{N_B} \cdot ln\Phi_B\right)$ Equation 1. 1 describes the enthalpy of the block copolymer, while the second part of the $\Delta G_{mix} = K_B T \cdot \chi_{AB} \cdot \Phi_A \cdot \Phi_B + K_B T \cdot \left(\frac{\Phi_A}{N_A} \cdot ln\Phi_A + \frac{\Phi_B}{N_B} \cdot ln\Phi_B\right)$ Equation 1. 1 demonstrates the entropy of the block copolymer.

Therefore, the enthalpy term results in positive Gibbs energy which leads to demixing of the copolymers. At the same time, the demixing process generates segregation between the building blocks which stretches the polymer chain out and thus leads to negative entropy (in other words, negative Gibbs energy) and affects the trend to mix. However, the enthalpy part is relatively more important than the entropy part, for the large degree of polymerization decreases the importance of the entropy part [32][33][34].

The interaction between the enthalpy and entropy parts in the Gibbs free energy equation results in interface formation and depends on the product of $\chi_{AB}N$. Traditionally, $\chi_{AB}N \leq 10$ results in weak phase separation, also termed as the weak segregation limit (WSL), while

$\chi_{AB}N \gg 10$ results in strong phase separation, in the so called strong segregation limit (SSL) [1].

The Bates group has depicted a more detailed explanation about interface formation by different degrees of order [35]. Assuming the block copolymer is comprised of 50% of each block, the resulting scheme is simulated as shown in Figure 1. 4. For $\chi_{AB}N \ll 10$, entropic factors predominate and block copolymers show a spatially homogeneous state. If χ_{AB} or N increase, the free energy balance would shift to form local composition fluctuations. As $\chi_{AB}N \approx 10$, the entropy and enthalpy achieve a critical balance. If further increasing χ_{AB} or N, there would appear a first-order transition to reach an ordered state, which means the disordered microstructures are substituted by the periodic mesophase. This phase transition is termed the order-disorder transition (ODT). Continuing to increase $\chi_{AB}N$ would lead to sharper microstructure boundaries, since the contact of A-B blocks decreases at the expense of additional chain stretching. When $\chi_{AB}N \gg 10$, enthalpy dominates, and thus the ordered microstructures are depicted as narrow interfaces and flat composition profiles.

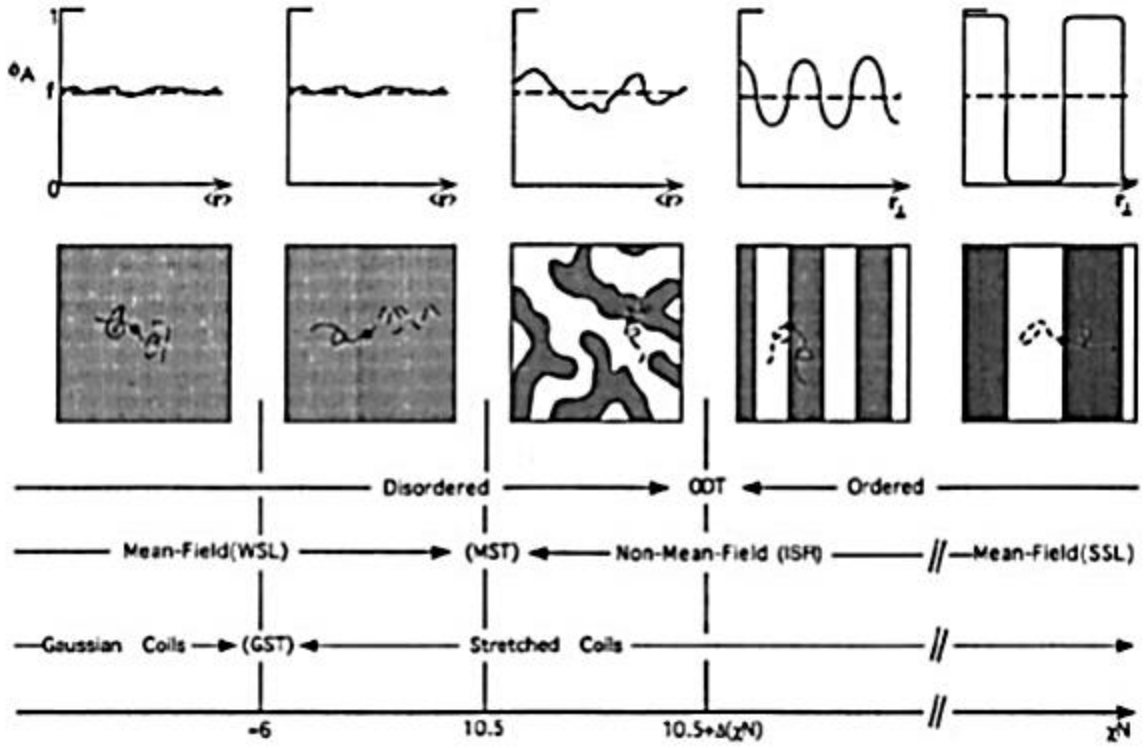

Figure 1. 4 Evolution of structure with the combined parameter for a symmetric diblock copolymer with f=0.5 [35].

Processed block copolymers are often not in thermodynamic equilibrium, such as spin-coating and drop-casting. The microstructure is always affected by the solubility of the blocks and thus resembles that of a solution [36]. Therefore, it is preferred to anneal the block copolymer after processing in order to encourage longe range order. One common but important method is to introduce solvent molecules to improve the mobility of the blocks. The interaction parameter χ is the standard to distinguish good ($\chi < 0$) , theta ($\chi = 0.5$) and poor ($\chi > 0$) solvents. For most cases, the solvents have different interactions between the blocks in copolymers. In other words, the blocks will swell to a different degree, and thus the volume fraction of the blocks in copolymer will change. Consequently, it is possible to reach different phases by altering the solvents, to achieve asymmetric swelling and/or shrinking [37][38].

1.4 Grignard metathesis

Thiophene was first found and extracted for study as a substance contained in coal-tar benzene in 1883 [39]. During 1884 – 1980, there existed numerous studies of polymerization of thiophene material. Meyer obtained amorphous, highly insoluble oligomer thiophene by sulfuric acidic materials [40]. Later on, Meisel et al. used 100% orthophosphoric acid, activated montmorillonite clays and synthetic silica-alumina catalysts to successfully produce liquid polymers of thiophene and alkylthiophenes, predominantly trimers with smaller amounts of pentamers [41]. Armour et al. made use of trichloro- and trifluoroacetic acid as catalyst to produce cyclic polythiophene containing a short sequence of double bonds, which resulted as colored properties [42]. Ramsey et al. reported for the first time that polythienylenes could couple through the 2,3-positions, by using aluminum chloride - cupric chloride in carbon disulfide under mild conditions. And the mechanism underneath was nuclear coupling by dehydrohalogenation [43]. Based on previous studies, Curtis et al. produced 2,4-di-2-thienyltetrahydrohiophen as *cis*- and *trans*- isomers and 4,7-di-2-thienyl-1,2,3,4-tetrahydrobenzo thiophene by polyphosphoric acid [44].Tourillon et al. used electrochemical oxidation methods to synthesize polythiophene, together with a new class of conducting polymers, such as polypyrrole, polyfuran, polyindole, polyazulene, etc., by the use of platinum or other metals [45]. However, only oligomers containing three to five repeating units could be produced by using all these synthesis methods demonstrated above.

Aiming at higher molecular weight during synthesis of polythiophene, the Yamamoto Group first achieved longer polymer chains containing many more repeating units than previous trials made by other researchers [46]. They used a 1:1 molar ratio of 2,5-

dibromothiophene and magnesium metal, and took advantage of [$NiCl_2$(bpy)], a transition metal catalyst, to successfully produce high molecular weight polythiophene. The main drawbacks of this attempt are insolubility and non-controllability of positions of coupling.

During optimization of synthesis of polythiophene, the Yamamoto Group discovered a monomer with alkyl chains substituted in the β-position of the thiophene ring, and 2,5-dibromo-3-alkylthiophene monomer, could be polymerized into a more soluble product with even higher molecular weight compared with previous non-substituted polythiophenes [47]. The shortcoming for this method is that the regioregularity of polymer chain cannot be controlled.

In 1992, the McCullough Group and the Chen and Rieke Group made significant breakthroughs in producing regioregular poly(3-alkylthiophene) [48][49]. They adopted lithiation followed by Kumada cross-coupling polymerization using highly activated metallic zinc reagent or Negishi coupling polymerization respectively. The disadvantage in both methods is the same, the requirement of cryogenic temperatures during polymerization. In 1999, the McCullough Group optimized their synthesis procedure at reflux conditions instead of cryogenic temperatures to produce regioregular polythiophene much more conveniently [50].

It is very important to understand the mechanism of polymerization, and thus take advantage of it to explore brand-new polymers. During the very first step of chemical polymerization of 3-alkylthiophenes, a Grignard coupling is produced by reaction between 2,5-dihalo-3-alkylthiophene and Grignard reagent, which termed as Grignard metathesis (GRIM).

At the very beginning of the polymerization mechanism study, the Kumada Group proposed a transmetallation concept as a first step mechanism and step-growth mechanism as a whole, which stated the polymerization is a polycondensation reaction with uncontrolled molecular weight and large PDIs [51]. However, the Yokozawa Group demonstrated that the Mn reached at the end of reaction was directly proportional to the ratio of monomer to catalyst, with controlled molecular weight and narrow PDIs, which certified the GRIM as a chain-growth mechanism [52].

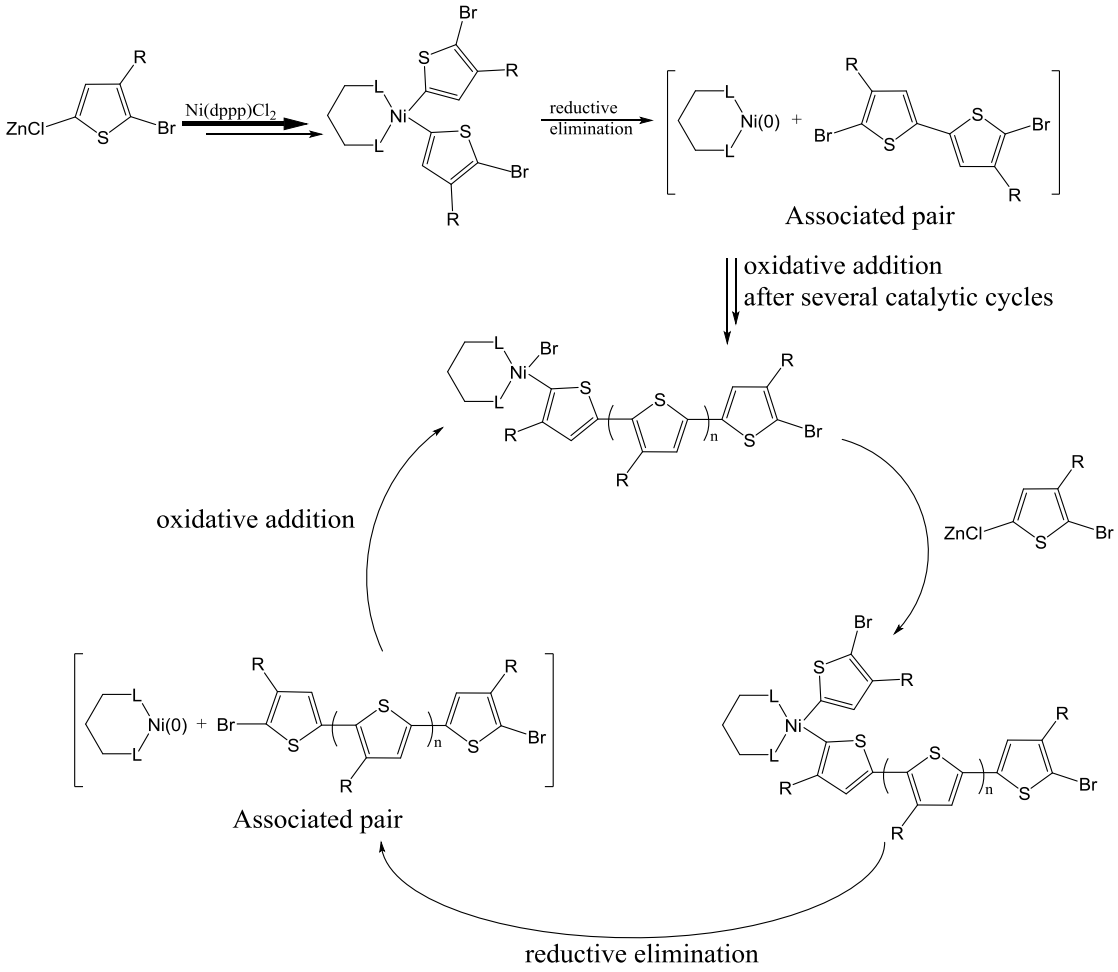

Figure 1. 5 Chain-growth mechanism of Grignard metathesis polymerization proposed by the McCullough group [53].

Later on, the McCullough group also claimed a chain-growth mechanism for GRIM as two steps: (1) transmetallation reaction underwent between two molecules of 2-bromo-5-chlorozincio-3-hexylthiophene or 2-bromo-5-chloromagnesio-3-hexylthiophene and Ni(dppp)Cl_2 catalyst molecule and (2) reductive elimination to form TT coupled 5,5'-dibromo-4,4'-dihexylbithiophene and a Ni(0) complex [53]. It forms an associated pair between the nickel catalyst and the polymer chain, with nickel catalyst involved in a further oxidative addition reaction, and followed by nickel group removal from the polymer chain by reductive elimination, as shown in Figure 1. 5.

The McCullough Group further stated that GRIM polymerization was a quasi-living reaction, for the polymer chains were active at the end of the reaction and could be end-capped by active Grignard reagent [54].

1.5 Atom transfer radical polymerization

In polymer synthesis chemistry, many interests have been put into the synthesis of well-defined compositions, architectures, and functionalities polymers. Living polymerization attracts great attention since the polymerizations takes place in the existence of irreversible chain transfer and chain termination [55]. At the beginning, research groups focused on anionic, cationic, coordination and ring-opening living polymerizations, and only recently, the controlled/living radical polymerization (CRP) has been realized, with its advantages in more tolerance functional groups and impurities [56]. During the past few years, CRP methods have grown rapidly, whose mechanism is based on a rapid dynamic equilibrium between a minute amount of growing free radicals and a large majority of the dormant species. The polymerizing chains might be alkyl halides, as in atom transfer radical polymerization (ATRP)

or degenerative transfer (DT), thioesters, as in reversible addition fragmentation chain transfer processes (RAFT), alkoxyamines, as in nitroxide mediated polymerization (NMP) [57].

A general mechanism for transition metal catalyzed ATRP is shown in Figure 1. 6. The radicals are generated via a reversible redox process by a transition metal complex (M_t^n-Y/Ligand) which undergoes a one-electron oxidation by elimination of halogen atom, X, from a dormant species, R-X. This process is controlled by a rate constant of activation, K_{act}, and deactivation K_{deact}. Polymer chains grow by the addition of intermediate radicals to monomers with the rate constant of propagation K_p. Termination reactions occur via radical coupling and disproportionation, with the rate constant of termination K_t. A traditional ATRP has a uniform growth of all the polymer chains with only a small amount of terminated chains, which is accomplished through fast initiation and rapid reversible deactivation [58].

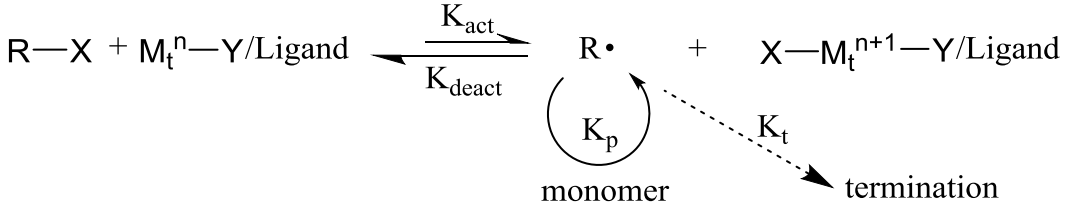

Figure 1. 6 Scheme of transition-metal catalyzed atom transfer radical polymerization (ATRP).

The development of ATRP includes the design of an appropriate catalyst, such as a transition metal compound and ligand; the use of an appropriate initiator; the optimization of the polymerization conditions, to have the molecular weights increase linearly with low polydispersities [59]. Therefore, as a multicomponent system, ATRP is composed of the monomer, the initiator with transferable halogen, the catalyst composed of a transition metal with suitable ligand, solvent appropriate for a specific system, and the temperature which could lead to successful reaction.

For monomers, typical examples include styrenes, (meth)acrylates, (meth)acrylamides, and acrylonitrile. Every monomer has its own unique atom transfer equilibrium constant for its active and dormant species, so each reaction system should be considered specifically. For initiators, the key role is to determine the number of growing polymer chains. The theoretical degree of polymerization (DP) is negative correlation with the amount of initiators (DP = $[M]_0$ / $[initiator]_0$ * conversion). When the initiating moiety is attached to macromolecular species, macroinitiators are formed and thus could be used to synthesize block and/or graft copolymers [60]. For catalysts, it plays the most important role in ATRP, since it determines the equilibrium and dynamics between the dormant and active species. Several prerequisites have been settled for the catalysts, such as the metal center must have at least two oxidation states separated by one electron; the metal center should have good affinity to a halogen; the ligand should complex the metal strongly, and etc. [58]. For solvents, various kinds of solvents could be used for different monomers, such as benzene, toluene, acetone, dimethyl formamide. Several factors affect solvent choice. Chain transfer to solvent should be minimal. Additionally, the interactions between solvent and catalyst should be taken into account, as well as the solvent-assisted side reactions [61]. For temperature, the rate of polymerization in ATRP is positively correlated to temperature. In detail, the increase of temperature results in an increase of both radical propagation rate and atom transfer constant. On the other hand, chain transfer and other side reactions become more obvious at elevated temperatures [62]. Therefore, the optimal temperature depends largely on the monomer, the catalyst and the targeted molecular weight. For reaction time, elongated time leads to complete monomer conversion without increase of the polydispersity, but will result in loss of end groups [63].

ATRP of methyl methacrylate (MMA) has attracted great attention, for the facile processibility and the large range of available catalysts for the reaction. Since MMA ATRP has high value of equilibrium constants and easily to activate dormant species, higher dilution and lower catalyst concentration should be used for MMA polymerization. Specifically speaking, typical radical concentration for polymerization is estimated to be between 10^{-7} and 10^{-9} M. And most polymerizations are carried out in solution at temperature in the range of 70 to 90 ^{o}C [58].

Chapter 2 Experiments of diblock copolymer synthesis

2.1 Introduction

In this chapter, we introduce the materials used in synthesis, sample preparation for characterization, the instruments used for evaluating polymer properties, and the general routes used for preparation of the stable radical block copolymers.

Previously, stable radical polymers attracted attention from various research groups for their unique structure with an unpaired electron. As a result, there are many researchers focusing on their electron properties and the related applications [31]. However, rare study topics are about the fundamental mechanisms underneath the stable radical polymers applied in energy storage. Therefore, we designed a diblock copolymer with conjugated polymer block with stable radical polymer block, where conjugated polymer block, as well as the desired micro phase separation, provide better pathway for electron transportation.

In this study, poly(3-hexylthiophene) (P3HT) was chosen for the its high regioregularity as the conjugated polymer block. This head-to-tail coupled thiophene structure demonstrates superior performance that could be achieved by GRIM metathesis polymerization[64]. Another reason to select this conjugated polymer is that the end functional group of P3HT could be modified by *in-situ* termination with Grignard reagent at the end of polymerization, and thus further functionalization can be employed to synthesize block copolymers [22][25].

Poly(2,2,2,6,6-tetramethyl-4-piperidinyloxymethacrylate) (PTMA) is a typical nitroxide radical polymer, which composed is of a methacrylate backbone grafted with 2,2,6,6-tetramethylpiperidin-1-oxyl (TEMPO). TEMPO is highly stable under ambient atmospheric circumstances, owing to its resonance stability and steric protection afforded by its four

methyl groups. During charging processes, the nitroxide radical (N-O•) is oxidized to an oxoammonium cation (N+=O). During the discharging process, the oxoammonium cation is reduced back to a nitroxide radical. The redox reaction between the oxoammonium cation and the nitroxide radical is completely reversible [30].

Poly(3-hexylthiophene)-*block*-Poly(2,2,6,6-tetramethyl-4-piperidinyloxymethacrylate) (P3HT-b-PTMA) was synthesized by polymerizing P3HT to form a macro-initiator as the first step, through modification of McCullough's already established methods, then the second block was attached to the initiator by using optimized ATRP methods, and finally the amine groups were oxidized to nitroxide radicals via established methods [65]. Block copolymers with different molecular weight ratios were synthesized, to understand the relationship between the difference in molar ratio and the corresponding change in microstructure and resistance properties. The purification process was chosen on the basis of the polarity and solubility of impurities in common solvents. Physical characterization was conducted to ensure every step was fully reacted and excess impurities were successfully removed, and to study the microstructures of the polymers and their related conductivity properties.

2.2 Materials

2,5-dibromo-3-hexylthiophene (> 98% purities) was purchased from Ark Pharm. 2,2,6,6-tetramethyl-4-piperidyl methacrylate was purchased from TCI America. Butyl magnesium chloride (*b*-MgCl), vinyl magnesium bromide, [1,3-Bis(diphenylphosphino)propane]dichloronickel(II) ($Ni(dppp)Cl_2$), 9-borabicyclo[3,3,1]nonane solution (9-BBN), triethylamine, α-bromoisobutyryl bromide (BIBB), 1,1,4,7,10,10-hexamethyltriethylenetetramine (HMTETA), Copper(I) bromide (CuBr), 3-chloroperbenzoic

acid (mCPBA) were purchased from Sigma-Aldrich and used without further purification unless otherwise noted. Tetrahydrofuran (THF) and toluene were purchased from Fisher Scientific. THF was distilled with the mixture of sodium and benzophenone and stirred at 85 ℃ for 4 hours, starting from the color of solution becoming deep purple before use. CuBr was purified by stirring in acetic acid, washing with methanol then drying.

2.3 General methods

Molecular weight and dispersity (PDI) of all samples were measured by gel permeation chromatography (GPC), using a Waters Ambient-Temperature GPC, equipped with a Waters 410 differential refractive index detector, a Waters 486 UV-Vis detector, and a Wyatt Technologies TREOS three-angle light-scattering detector. The samples were all prepared at 1 mg/mL in THF and filtered before use.

^{1}H nuclear magnetic resonance (NMR) was recorded on either a Varian Gemini 300 MHz, or a Varian Gemini 400 MHz with deuterated chloroform, chemical shifts (δ) were reported in parts per million (ppm) relative to tetramethyl silane (TMS). The samples were prepared at ~1 wt.% in $CDCl_3$.

Atomic force microscopy (AFM) was performed from Veeco (TM) Instruments Inc. / Bruker AXS GmbH. All images were taken under TappingMode in air. The polymer thin films were spin-coated and/or drop-casted onto glass substrates for AFM imaging. The substrates were dried and cleaned with nitrogen before use. The polymer solutions (10 mg of polymer per 1 mL of good solvent) were spin-coated at a rotational rate of 2000 rpm for 60 s with acceleration of 800 rpm/s, and then annealed under the same solvent vapors at room temperature for 24 hours. This spin-coated procedure led to the formation of ~ 100 nm thick

films. The solutions (0.02 vol.% in good solvent) were drop-casted to the substrate and then annealed under the same solvent vapors at room temperature for 24 hours. This drop-casted procedure led to the formation of 20 to 50 nm thick films.

Thermogravimetric differential thermal analysis (TG/DTA) was performed on Seiko Instruments TG/DTA 6200 with nitrogen purging. The samples were annealed from 25 to 600 ℃ at a scan rate of 10 ℃/min, and held at 600 ℃ for 5 min.

Ultraviolet-visible spectroscopy (UV-vis) was performed on Molecular Devices of model Spectramax MLe. The samples were pre-dissolved in chloroform with the concentration of 1 wt. %. The experiment was carried out from 300 to 600 nm wavelength with the step of 10 nm wavelength.

Electron Paramagnetic Resonance (EPR) was performed on an X-band Bruker ELEXSYS E500 CW-EPR Spectrometer, was radio frequency (RF) of 9.44 GHz. Stable radicals have long been used as molecules to obtain structural, dynamic, and reactivity information through EPR. A small molecule, 4-hdroxy-2,2,6,6-tetramethylpiperidin-1-oxyl (TEMPO-OH) was used as the standard sample. All the samples were prepared at 0.5 mmol/L in chloroform by spin concentration at room temperature.

Resistance testing was performed with highly-sensitive devices with two 2 mm length of gold wires with the separation distance of 2 um, on a pretreated silica substrate. The height of cross-section is the thickness of the coating polymer films. Figure 2. 1 shows the scheme of the test device.

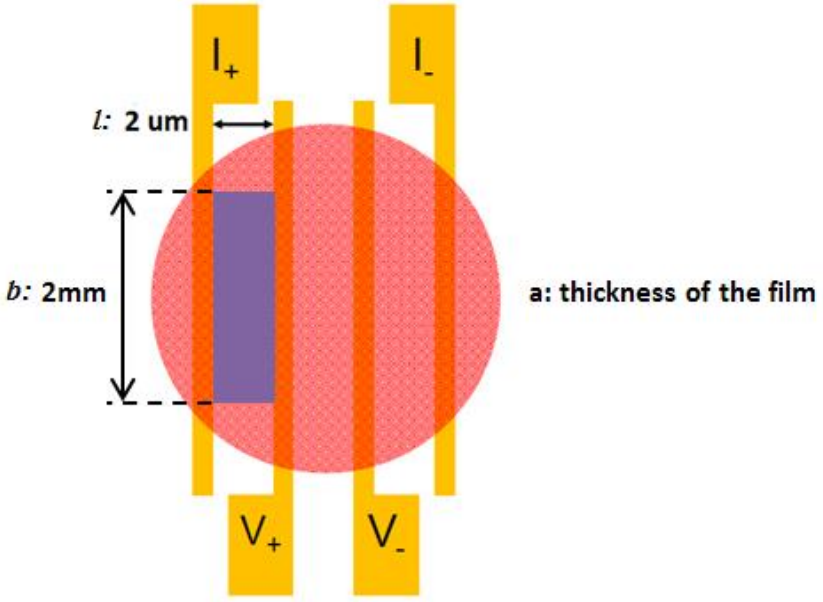

Figure 2. 1 Top view of the scheme of the test resistance test device

Film thickness was obtained through Tencor Alpha Step 500 for the measurements.

2.4 Exemplary synthesis routes

A simplified synthesis procedure is shown schematically in Figure 2. 2. All diblock copolymers were synthesized by using a McCullough GRIM polymerization and an ATRP mechanism where the P3HT-Br served as the macroinitiator. The molecular weight of the PTMA unit was controlled by changing the molar ratio of the monomer to the macroinitiator. An exemplary P3HT-PTMA diblock copolymer synthestic procedure is shown in detail below.

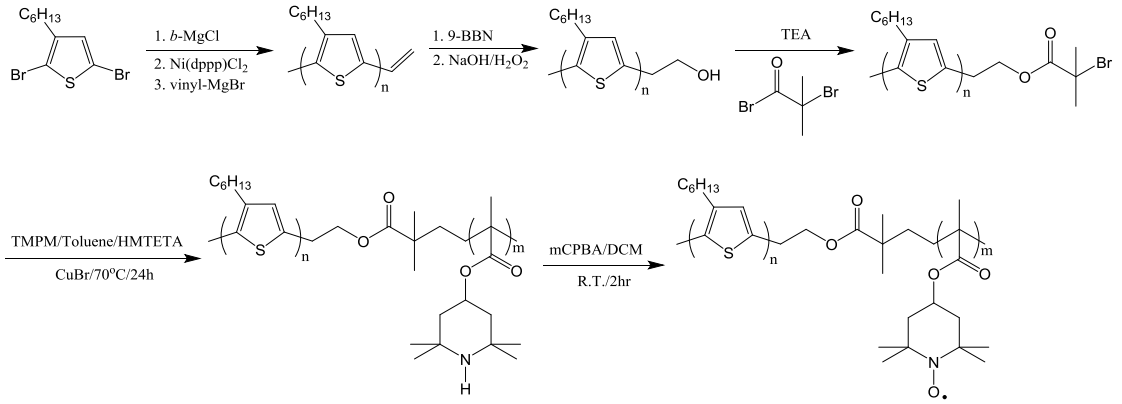

Figure 2. 2 Synthetic procedure of poly(3-hexylthiophene)-block-poly(2,2,6,6-tetramethyl-4-piperidinyloxymethacrylate) (P3HT-*b*-PTMA)

Vinyl terminated P3HT (1) 2,5-dibromo-3-hexylthiophene (2 g, 6.12 mmol) and anhydrous THF (60 mL) were added to a dry 100 mL round-bottom flask under N_2 atmosphere. A 2M solution of butyl magnesium chloride (3.1 mL, 6.12 mmol) in diethyl ether (Et_2O) was added to the flask. A clean, dry stir bar was then placed in the flask and the reaction mixture was gently stirred for 24 hours, until the color of the solution changing from colorless to light yellow. The Ni(dppp)Cl_2 (61.2 mg, 0.11 mmol) was added to the reaction mixture, at which time the polymerization took place. The color of the reaction mixture turned rapidly to bright orange. A time of 15 min was allowed for the polymerization at room temperature. Then a 1M solution of vinyl magnesium bromide (1.2 mL, 1.22 mmol) in THF was added to the reaction solution and stirred for another 5 min. The color of the reaction mixture became somewhat darker. The reaction was stopped by quenching the solution in 1 M HCl. The polymer was filtered and purified by sequential Soxhlet extractions with methanol, hexanes, and chloroform. The polymer was isolated from the chloroform solution. The synthesis procedure is shown schematically in Figure 2. 3.

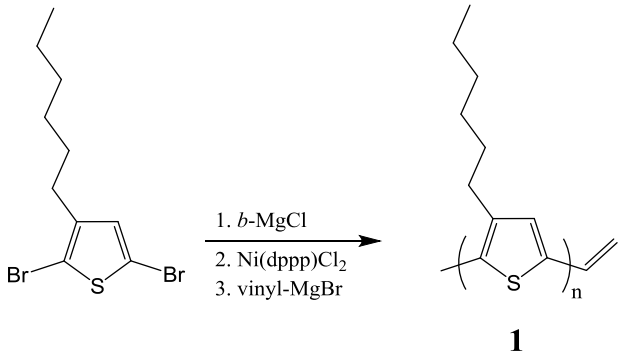

Figure 2. 3 Synthesis scheme of vinyl terminated poly(3-hexylthiophene).

Hydroboration of vinyl terminated P3HT (2) **1** (750 mg, 0.075 mmol), anhydrous THF (100 mL) and a stir bar were added to a dry 250 mL round-bottom flask under N_2 atmosphere. The solution was stirred rapidly until all solids dissolved. A 0.5M solution of 9-BBN (2.25 mL, 1.13 mmol) in THF was added to the flask by syringe. The reaction system was stirred gently under N_2 atmosphere at 40 ℃ for 24 hours. The oil bath was removed and the reaction mixture allowed to cool down to room temperature, at which point a 6 M solution of NaOH (2.3 mL) was added to the flask. The reaction mixture was stirred for 5 min at room temperature. A 30% aqueous solution of hydrogen peroxide (1.2 mL) was added dropwise to the reaction mixture. Each time the droplet touched the solution surface, there appeared deep purple aggregation. The mixure was stirred until all aggregation re-dissolved into the solution and then another droplet was added. Eventually a precipitated white salt would appear at the bottom of the flask. The reaction system was stirred at 40 ℃ for 24 hours. The hydroxyl terminated P3HT was isolated by precipitation in a methanol-water mixture. The polymer was filtered and purified by sequential Soxhlet extractions with methanol and chloroform. Finally the polymer was isolated from the chloroform solution. The synthetic procedure is shown schematically in Figure 2. 4.

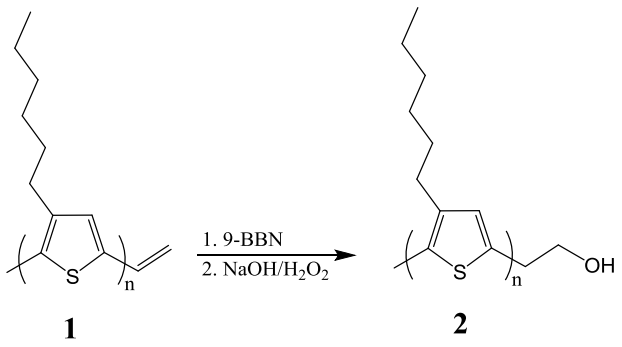

Figure 2. 4 Synthesis scheme of hydroxy terminated poly(3-hexylthiophene)

Bromine terminated P3HT macroinitiator (3) **2** (700 mg, 0.07 mmol), anhydrous THF (100 mL) and a stir bar were added to a dry 250 mL round-bottom flask under N_2 atmosphere. The mixture wa stirred rapidly until all solids dissolved. Triethylamine (6.9 mL, 50 mmol) was added to the reaction mixture by syringe. Then α-bromoisobutyryl bromide (5.8 mL, 46 mmol) was added dropwise to the flask. The reaction mixture was stirred gently at 40 ℃ for 24 hours. The polymer was filtered and purified by Soxhlet extraction in methanol. The synthetic procedure is shown schematically in Figure 2. 5.

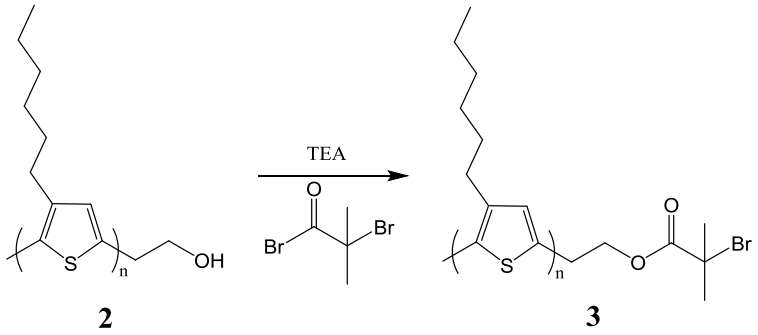

Figure 2. 5 Synthesis scheme of bromine terminated poly(3-hexylthiophene)

P3HT-b-PTMPM (4) The second block of poly(2,2,6,6-tetramethyl-4-piperidyl methacrylate) (PTMPM) was added to P3HT macroinitiator using ATRP. 2-bromo-2-methyl P3HT macroinitiator (**3**) (172 mg, 0.017 mmol), TMPM (775 mg, 3.4 mmol), HMTETA (10.8

uL, 0.051 mmol), toluene (10 mL) and a stir bar were placed in a 25 mL Schlenck flask (I). The reaction was stirred rapidly until all the solids dissolved. The reaction solution was frozen by immersing the reaction vessel into a dewar with liquid nitrogen until all the solution became solid. A vacuum was applied to the Schlenck flask over 5 min. The valve on the Schlenck flask was closed and the reaction mixture thawed by immersing the flask into a dewar with room temperature water. This freeze-thaw step was repeated for 3 to 5 times until dissolved air in the reaction solution was pumped out. CuBr (2.5 mg, 0.017 mmol) and a stir bar were added to a 25 mL Schlenck flask (II). The flask was bubbled through with nitrogen for 15 min. The reaction mixture in a Schlenck flask (I) was cannulated over to a second Schlenck flask (II). The freeze-thaw process was repeated 2 times more on Schlenck flask (II). The reaction mixture was immersed in an oil bath at 70 ℃ for 24 hours. After 24 hours, the reaction was stopped by pouring the mixture into a beaker with aluminum oxide (neutral) and stirred overnight to remove the residual copper from solution. The solution was filtered using a glass funnel half-filled with aluminum oxide. Excess solvent was evaporated and the product was concentrated in a hexane solution. The resulting polymer was filtered and dried under reduced pressure overnight. At this point, there will have impurities from the TMPM monomer residuals. The synthetic procedure is shown schematically in Figure 2. 6.

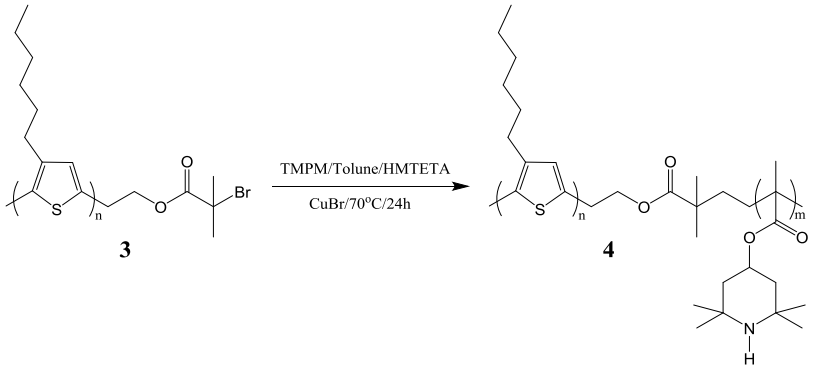

Figure 2. 6 Synthesis scheme of poly3HT-b-PTMPM

Next, the dried polymer powders were dissolved in THF, and the solution was injected into a dialysis tube (cut-off molecular weight of 1.2 kg/mol) and stirred at room temperature in 1L THF for 24 hours to remove residual monomer from the solution. 1L THF was changed every 24 hours and that solution was evaluated by FTIR to see if it was purified. Figure 2. 7 shows the FTIR spectrum for THF solutions used in dialysis before complete purification for P3HT-*b*-PTMPM. The complete purification of the diblock copolymer is indicated by complete disappearance of the broad peak at 3,300 wavenumbers due to the amine N-H bond.

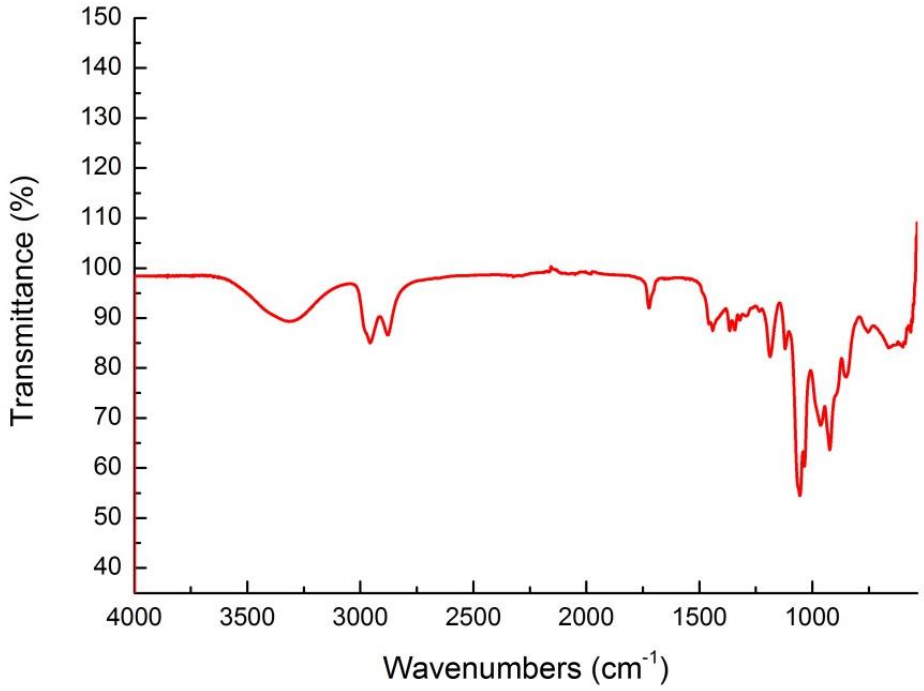

Figure 2. 7 FTIR spectrum of a THF solution used in dialysis before complete purification for poly(3-hexylthiophene)-*b*-poly(2,2,6,6-tetramethyl-4-piperidyl methacrylate) (P3HT-*b*-PTMA) diblock copolymer.

P3HT-b-PTMA (5) **4** (500 mg) was dissolved in dichloromethane (DCM, 10 mL). A separate solution of mCPBA (500 mg) was made in DCM (10 mL). The mCPBA solution was added to the polymer solution dropwise while under N_2 atmosphere and stirring at room temperature. The reaction was allowed to proceed for 2 hours. The reaction mixture was then

washed with aqueous sodium carbonate solution (20 wt.%) for at least 3 times. The collected solution was precipitated in hexanes. The resulting polymer was filtered and dried under reduced pressure overnight. The synthetic procedure is shown schematically in Figure 2. 8.

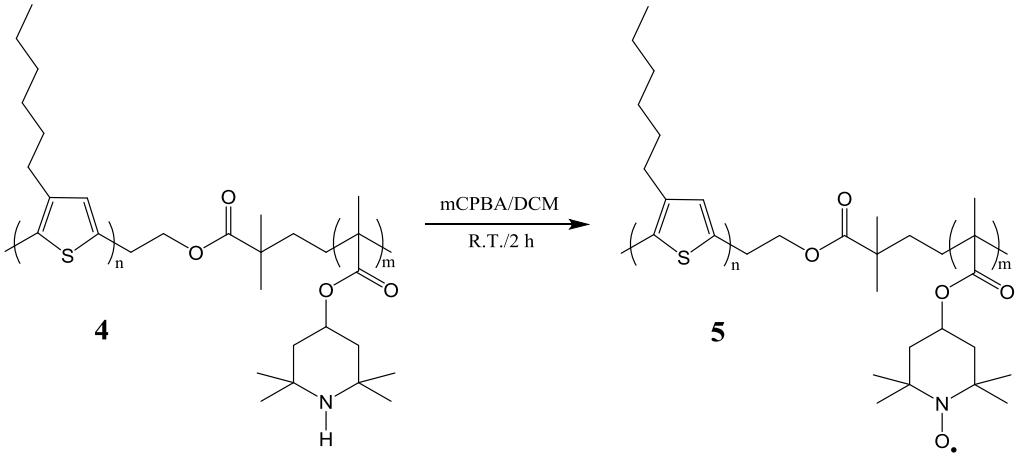

Figure 2. 8 Oxidization scheme of poly3HT-b-PTMPM to P3HT-b-PTMA

2.5 Detailed Experimental content

In order to study the relationship between the difference in block ratios and the corresponding change in polymer properties, different molecular weight ratios of P3HT and PTMPM blocks were achieved through quasi-living Grignard metathesis polymerization and atom transfer radical polymerization, by tuning the feed ratio of 3-hexylthiophene (3HT) monomer to nickel catalyst and the feed ratio of TMPM monomer to macro-initiator, respectively.

Table 2. 1 provides all the feed ratios of 3HT to nickel catalyst investigated in these studies. Table 2. 2 provides all the feed ratios of TMPM to macro-initiator made during this research program.

Table 2. 1 Different molar ratio used in Grignard metathesis polymerization to produce P3HT

	3HT molar ratio	Ni-cat. molar ratio	Target Mn (g/mol)
1	30	1	5,500
2	60	1	11,000
3	120	1	22,000

Table 2. 2 Different molar ratio used in atom transfer radial polymerization to produce PTMPM

	TMPM molar ratio	Macro-initiator ratio	Target PTMPM Mn (g/mol)
1	100	1	22,500
2	200	1	45,000
3	250	1	56,000
4	300	1	67,500

Chapter 3 Characterization of a block copolymer with both conjugated and TEMPO containing segments

3.1 Introduction

In this chapter, we evaluate the microstructure and electrical properties of our P3HT homopolymers and P3HT-*b*-PTMA diblock copolymers. While we achieved different molecular weights of P3HT homopolymers ranging from tens of repeat units to hundreds of repeat units, we further successfully produced different molecular weights of PTMA blocks attached to the P3HT blocks. In addition to the traditional NMR and GPC measurements to confirm our research products, the bathochromic shift of the absorption peak in the UV-vis spectra and the extreme changes of polymer color also confirm the outcome. In order to optimize the regioregular P3HT with higher polydispersity and more controlled molecular weights, we improved our quenching method from using methanol to hydrochloric acid, which resulted in an improvement in dispersity from around 1.3 to 1.1. The subsequent AFM phase images show that the P3HT with lower molecular weights align better in stripe-like structures than those with higher molecular weights. And the AFM phase images of P3HT-*b*-PTMA diblock copolymers reveal that different microphase separation is achieved depending on different solutions and film thicknesses, and ranges from stripe-like microstructure to hole-like microstructure. Our inspiration is to study the fundamental mechanisms underneath the radical group transport methods. We successfully obtained resistance parameters of P3HT conjugated polymers. However, the conductivity of our diblock copolymers was undetectable by our test equipment, so we proposed several device prototypes to better characterize this

property. Finally, we studied the conversion of the radical groups to further guarantee the resistance valudes of the block copolymers were effective and consistent.

3.2 Physical characterization results

3.2.1 NMR and GPC for poly(3-hexylthiophene)

^{1}H NMR spectroscopy is a universally used technique to study polymer structures based on the local molecular environment of hydrogen in a chemical structure. Here the ^{1}H NMR spectroscopywas conducted to ensure every reaction was take to completion and impurities were successfully removed.

Figure 3. 1 shows the ^{1}H NMR spectrum of vinyl terminated poly(3-hexylthiophene), which indicates the presence of vinyl protons at 5.1 ppm (peak a), 5.5 ppm (peak a) and 6.8 ppm (peak b). The presence of a thiophene-ring proton at 6.9 ppm (peak c) is high and sharp, which indicates success in the polymerization of P3HT. There are also indications for hexyl side chain protons at 2.7 ppm (peak d) and 1.2 ppm (peak e). Since there is only one proton at each peak a and peak c, the degree of polymerization (DP_n) of vinyl terminated P3HT

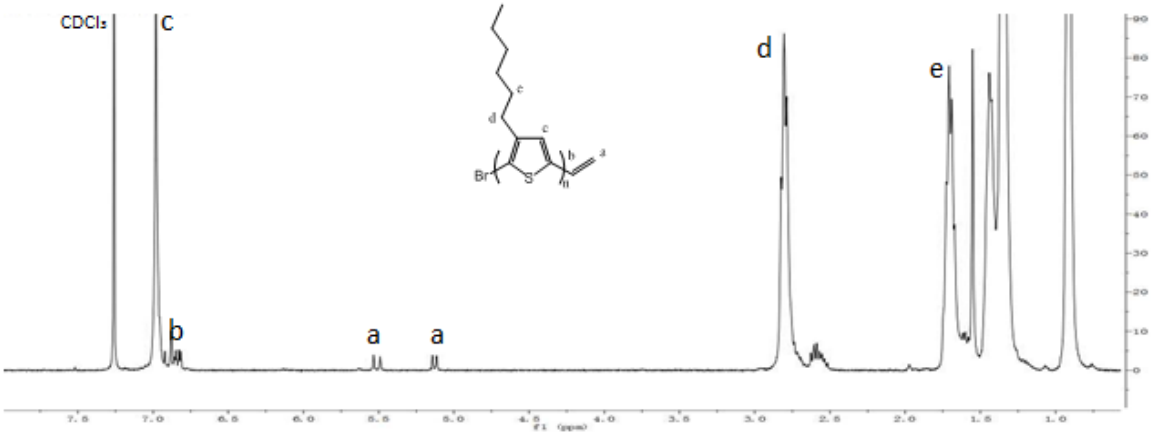

Figure 3. 1 ^{1}H NMR spectrum of vinyl terminated poly(3-hexythiophene)

could be estimated through integration of a protons compared to c protons from the ^{1}H NMR spectrum.

In Chapter 2.4, we mentioned that in order to study the relationship between the block ratios and the corresponding change in polymer properties, different molecular weights of the P3HT block should be achieved through Grignard metathesis polymerization, by tuning the feed ratio of 3-hexylthiophene (3HT) monomer to nickel catalyst. The final molecular weights of P3HT based on estimation through integration of a protons vs c protons from ^{1}H NMR spectrum. The obtained results are shown in Table 3. 1. As we can see from the table, the final molecular weights correspond well with the target molecular weights.

Table 3. 1 Different molar ratio used to produce P3HT and related final molecular weights

	3HT molar ratio	Ni-cat. molar ratio	Target Mn (g/mol)	Final Mn (g/mol)
1	30	1	5,500	6,000
2	60	1	11,000	11,500
3	120	1	22,000	23,000

Figure 3. 2 shows the ^{1}H NMR spectrum of hydroxyethyl terminated poly(3-hexylthiophene). The conversion of vinyl to hydroxyethyl terminated P3HT is indicated by the complete disappearance of vinyl protons and the appearance of new signals at 3 ppm (peak b), and 3.9 ppm (peak a) due to the methylene protons [66]. There are also thiophene-ring protons at 6.9 ppm (peak c) and hexyl side chain proton at 2.7 ppm (peak d).

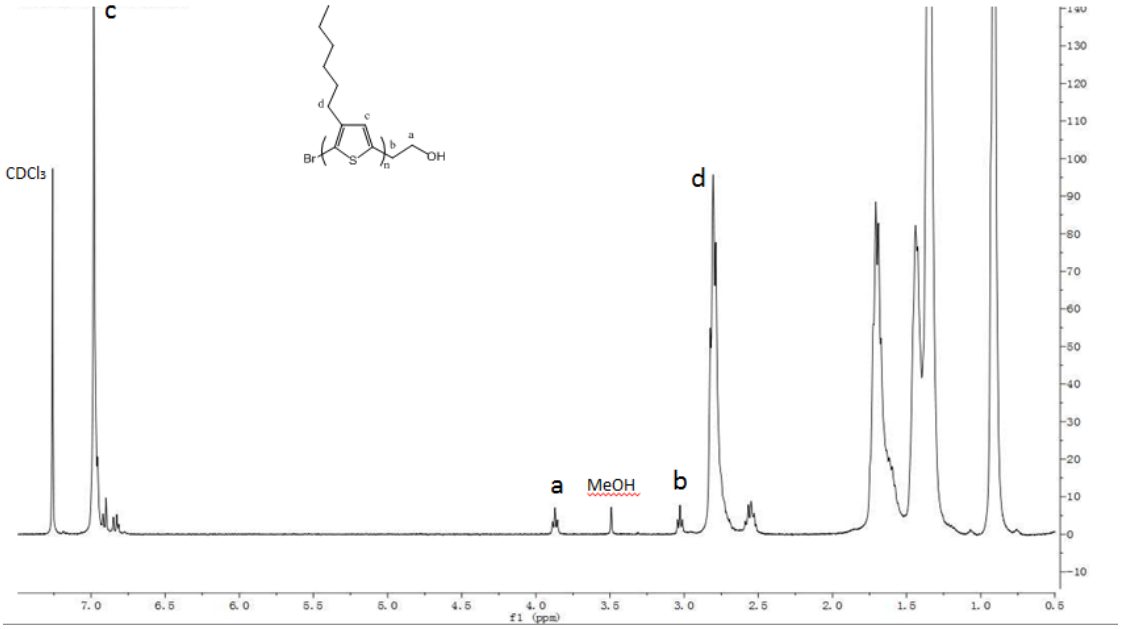

Figure 3. 2 ^{1}H NMR spectrum of hydroxyethyl terminated poly(3-hexythiophene)

Figure 3. 3 shows the ^{1}H NMR spectrum of the bromoester terminated poly(3-hexylthiophene). The conversion of hydroxyethyl to bromoester terminated P3HT is indicated by the complete disappearance of hydroxyethyl protons and the appearance of new signals of bromoester protons at 3.1 ppm (peak b), 4.4 ppm (peak a) due to the methylene protons. There are also thiophene-ring protons at 6.9 ppm (peak c) and hexyl side chain protons at 2.7 ppm (peak d).

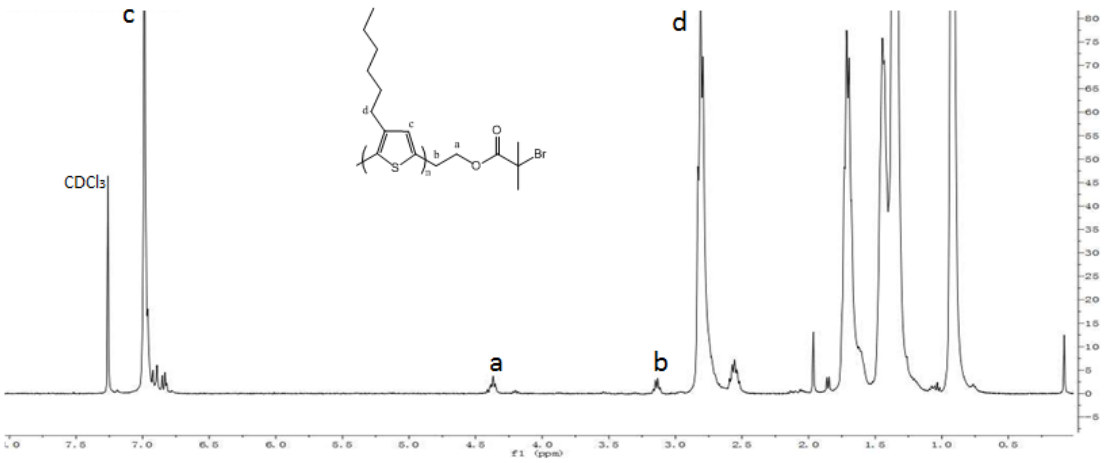

Figure 3. 3 ^{1}H NMR spectrum of bromoester terminated poly(3-hexythiophene)

Table 3. 2 shows the gel permeation chromatography (GPC) results of different molecular weights of poly(3-hexylthiophene), together with the target molecular weights and the resulting molecular weights estimated from ^{1}H NMR spectra. As can be seen from the table, the molecular weights of P3HT obtained from GPC are generally larger than those estimated from the integration of ^{1}H NMR spectrum.

Table 3. 2 Molecular weights obtained from GPC and the ones estimated from ^{1}H NMR spectrum.

	Target Mn (g/mol)	Mn integrated from NMR (g/mol)	Mn obtained from GPC (g/mol)
1	5,500	6,000	7,000
2	11,000	11,500	12,500
3	22,000	23,000	25,600

For the rod-like soluble polymers, such as P3HT, gel permeation chromatography (GPC) overestimates the molecular weight by the use of unmodified polystyrene (PS) calibration

procedures [67]. Because GPC measures the hydrodynamic volume of the polymer chains, calibrated to PS standards, it finally calculates their molecular weights based on PS calibration curves. It is reasonable to expect that there may be an overestimation of molecular weight for these rod-like polymers.

3.2.2. Optimization of controlled PDI for poly(3-hexylthiophene)

In previous chapters, we have demonstrated that the polymerization of 2,5-dibromo-3-hexylthiophene by Grignard metathesis polymerization is successfully carried out using a chain-growth condensation mechanism, which results in a high regioregular head-to-tail poly(3-hexylthiophene) with low polydispersity and controlled molecular weights.

However, the GPC profiles of the synthesized vinyl terminated P3HT (and/or hydroxyethyl terminated P3HT, bromoester terminated P3HT) show a small shoulder in the higher molecular weight region, as shown in Figure 3. 4 (a). Moreover, the molecular weights of the shoulder peaks are almost double those of the main peaks, which may due to a combination of polymer chains.

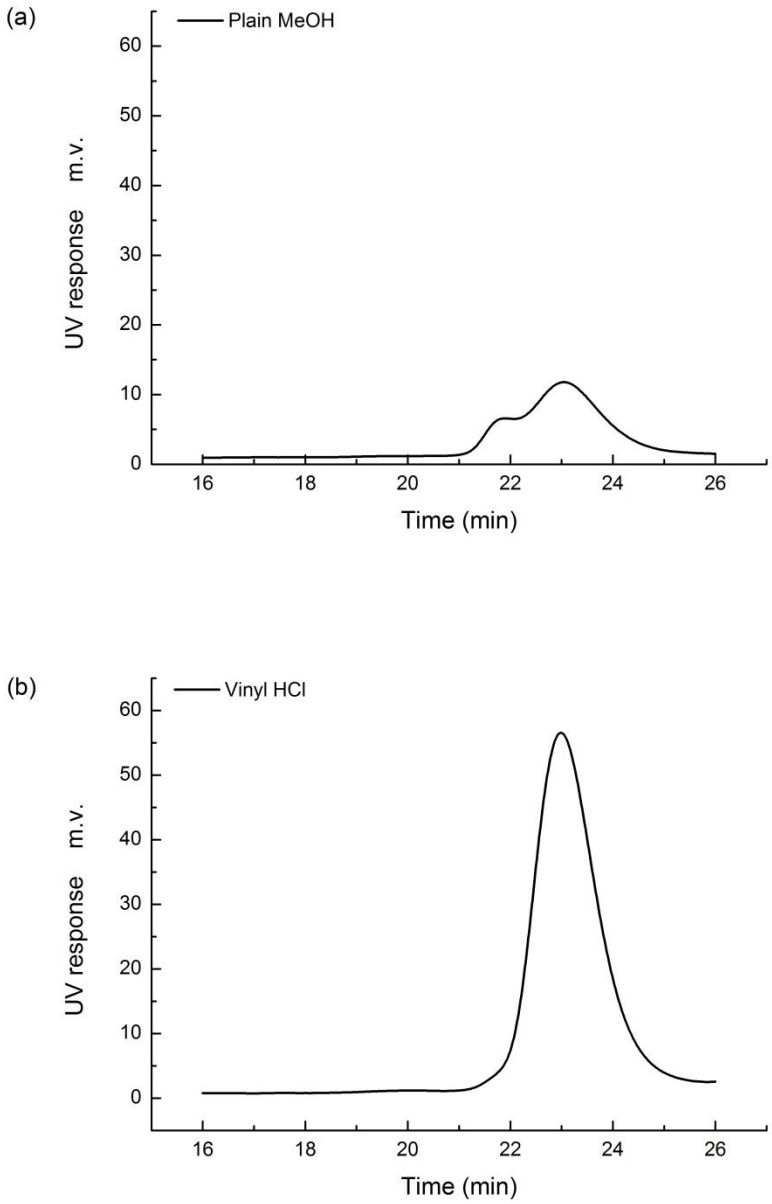

Figure 3. 4 GPC profiles of poly(3-hexylthiophene) obtained after quenching with methanol (a) and 1 M hydrochloric acid (b), respectively.

The Yokozawa group reported the same problem [68]. They examined the effect of quenching reagents on the polymerization. Their GPC profiles of polymers obtained by quenching with water were shown to be bimodal from the beginning of polymerization. While

the polymers obtained by quenching with hydrochloric acid showed unimodal, narrower molecular weight distribution. They proposed that the formation of a small amount of polymer with a higher molecular weight by quenching with water is accounted for by disproportionation of the P3HT-Ni(II)-Br complex, followed by reductive elimination of P3HT-P3HT as part of a combination reaction. The disproportionation may be caused by a change of the ligand of the P3HT-Ni(II)-Br complex when water is added into the reaction mixture. While quenching with hydrochloric acid, protonolysis is promoted before disproportionation of before reductive elimination. The similar effect of quenching reagents on the polydispersity of polymers obtained with a Ni catalyst was also investigated by the Yamamoto group [69].

Referred to the Yokozawa method, a successful synthesis of P3HT with a narrower polydispersity without any shoulder is achieved by quenching the polymerization with 1M hydrochloric acid instead of methanol, as shown in Figure 3. 4 (b).

3.2.3. NMR and GPC for poly(3-hexylthiophene)-block-poly(2,2,6,6-tetramethyl-4-piperidinyloxymethacrylate)

Figure 3. 5 shows the ^{1}H NMR spectrum of poly(3-hexylthiophene-*b*-poly(2,2,6,6-tetramethyl-4-piperidyl methacrylate) (P3HT-*b*-PTMPM). The success in addition of the PTMPM block to the macro-initiator is indicated by the complete disappearance of bromoester protons and the appearance of new signals at 5 ppm (peak b) due to the methine protons on the nitrogen-based six membered ring.

The composition of P3HT-*b*-PTMPM copolymers was estimated from the ^{1}H NMR spectrum, by integrating a protons (signals at 6.9 ppm) vs b protons, which represent the

degree of polymerization of polythiophene and the degree of polymerization of poly-TEMPO-methacrylate respectively. The results are shown in Table 3. 3. All of the diblock copolymers are synthesized from macroinitiators with molecular weights of 11,500 g/mol. The macro-initiators with molecular weights of 23,000 g/mol fail in the synthesis of the second blocks. There are two reasons mainly. Firstly, higher molecular weight macroinitiators are less soluble, and thus there will be larger impedance for the polymerization to take place. Secondly, higher molecular weight macroinitiators are more tangled in morphology, so it is harder for them to expose the bromine end-group to initiate ATRP process.

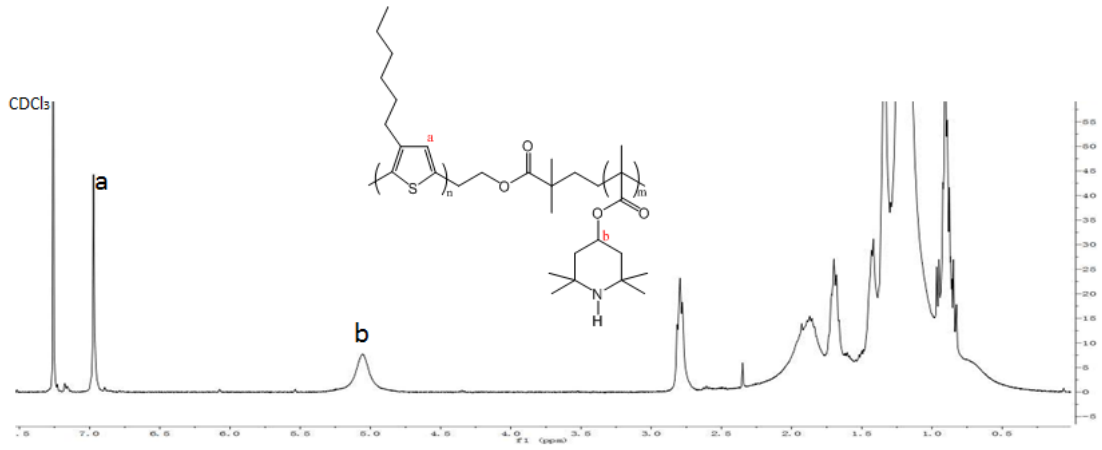

Figure 3. 5 ^{1}H NMR spectrum of poly(3-hexythiophene)-*b*-poly(2,2,6,6-tetramethyl-4-piperidyl methacrylate) diblock copolymers (P3HT-*b*-PTMPM).

Table 3. 3 Composition of poly(3-hexythiophene)-*b*-poly(2,2,6,6-tetramethyl-4-piperidyl methacrylate) diblock copolymers (P3HT-*b*-PTMPM) obtained from NMR.

	P3HT (mol%)	PTMPM (mol%)	Total Mn (NMR)
1	100	0	11,500
2	75	25	12,500
3	37	63	24,500
4	30	70	37,500
5	25	75	56,500

Another interesting observation to point out is that none of the refractive index (RI) and ultraviolet (UV) sensors in GPC could detect any trace of the P3HT-*b*-PTMPM diblock copolymers. This might because the amine groups on the PTMPM blocks interact with the columns of the GPC and become adsorbed.

Table 3. 4 shows the GPC results of different molecular weight ratios of P3HT and PTMA blocks, together with their total molecular weights and polydispersity. These GPC results indicate that, with the success in the oxidization of amine group into nitroxides, the P3HT-*b*-PTMA diblock copolymers will adhere to the columns of the GPC anymore.

Additionally, as can be seen from the table, the molecular weights of diblock copolymers with oxidized PTMA blocks are generally the same or a little bit larger than the unoxidized materials estimated from the integration of ^{1}H NMR spectrum. This makes sense because of the substitution of the amine groups with NO-centered nitroxides. And it is also reasonable that with a less than 100% yield of nitroxide formation in the PTMA block, there will be a broadening of the molecular weight.

There are no NMR analyses for the P3HT-*b*-PTMA diblock copolymers, since the nitroxides on the PTMA block will affect the spins of the atomic nuclei strongly, and thus result in uninterpretable results.

Table 3. 4 Composition of poly(3-hexythiophene)-*b*-poly(2,2,6,6-tetramethyl-4-piperidinyloxymethacrylate) diblock copolymers (P3HT-*b*-PTMA) obtained from GPC.

	P3HT (mol%)	PTMA (mol%)	Total Mn (GPC)	PDI (GPC)
1	100	0	11,500	1.29
2	75	25	12,500	1.38
3	37	63	25,000	1.75
4	30	70	38,000	1.77
5	25	75	57,000	1.88

Figure 3. 6 shows GPC traces of P3HT-*b*-PTMA copolymers with different molecular weights for the PTMA block. From this figure we can see that, the increase of the molecular weight of PTMA block corresponds well with the movement of the GPC peaks towards the longer retention time.

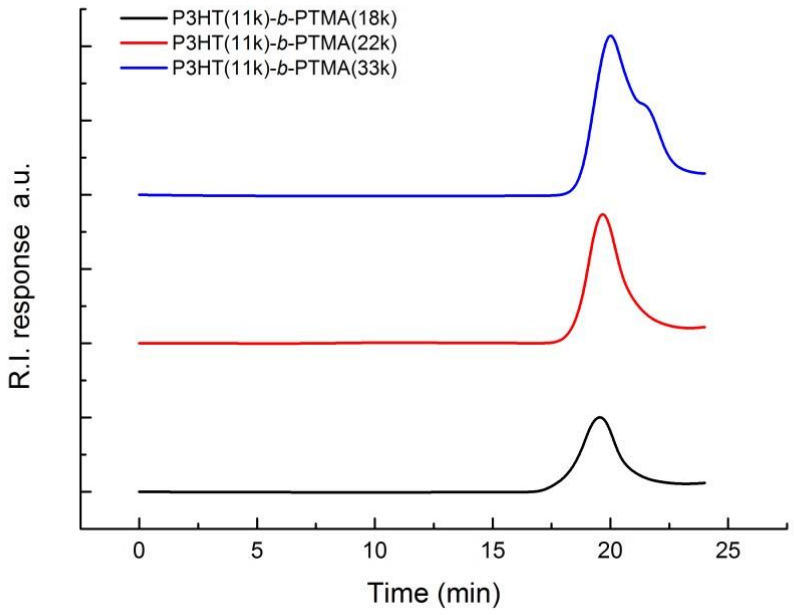

Figure 3. 6 GPC profiles of P3HT-*b*-PTMA diblock copolymer with different molecular weights of PTMA block.

There are interesting phenomena related to the color of diblock copolymers. Figure 3. 7 (a) shows the color of the pure poly(3-hexylthiophene) (P3HT), which is dark violet. In Figure 3. 7 (b), the color of the pure poly(2,2,6,6-tetramethyl-4-piperidinyloxymethacrylate) (PTMA) is yellow. Figure 3. 7 (c) shows the color of the P3HT-*b*-PTMA diblock copolymers with lower molecular weight ratios of PTMA, which more resembles that of the pure P3HT as violet, while Figure 3. 7 (d) shows the color of the P3HT-*b*-PTMA diblock copolymers with higher molecular weight ratios of PTMA, which more resembles that of the pure PTMA as yellow. Therefore, we could make a brief speculation of which block domains in the diblock copolymer chains just through the color of the polymer.

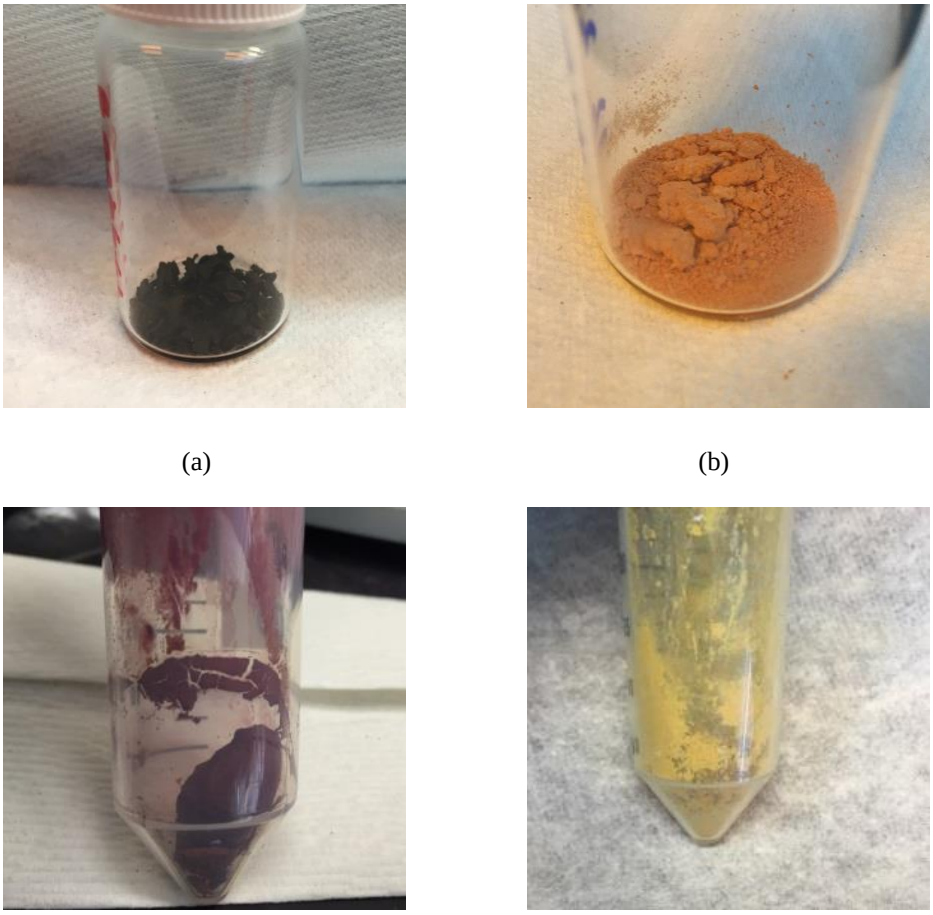

(a) (b)

(c) (d)

Figure 3. 7 Samples of (a) pure poly(3-hexylthiophene) (P3HT); (b) pure poly(2,2,6,6-tetramethyl-4-piperidinyloxymethacrylate) (PTMA); (c) P3HT-*b*-PTMA diblock copolymers with lower molecular weight ratios of PTMA; (d) P3HT-*b*-PTMA diblock copolymers with higher molecular weight ratios of PTMA.

3.3 Morphology characterization results

Since optical spectroscopy in solution can give information about the conjugation of isolated molecules, in the absence of interchain packing effects, we studied the absorption spectroscopies of different molecular weights of regioregular P3HT.

For regioregular P3HT, the conjugated length of a single chain is affected by the chain length. Figure 3. 8 shows the UV-vis spectra of regioregular P3HT in chloroform for three different molecular weight polymers produced by Grignard metathesis polymerization. The

number-average molecular weight of these P3HT segments is 6,000 g/mol, 11,500 g/mol, and 23,000 g/mol. From the graph we could see that, with the increase of molecular weight, there is a slight bathochromic shift of the absorption maximum, from about 440 to 450 nm. This may be accounted for by the increase in average conjugation length along the polymer backbone.

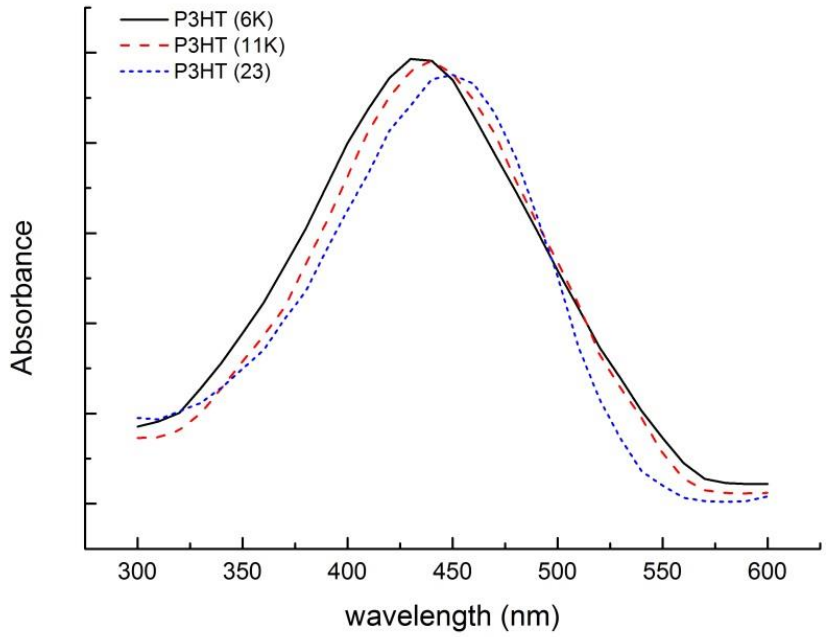

Figure 3. 8 UV-vis spectroscopy of P3HT at three different molecular weights in chloroform. The number-average molecular weight of these P3HT is 6,000 g/mol, 11,500 g/mol, 23,000 g/mol.

Aggregation in solution is accompanied by a dramatic color change from orange to violet. Figure 3. 9 is the photographic image of P3HT with 23,000 g/mol molecular weight in a toluene solution of 1 wt. % polymer at elevated temperature and room temperature, respectively. This phenomenon indicates a significant change in the physical conformation of the polymer chains. At room temperature, the polymer chains aggregate, as shown in Figure 3.

9 (a). With the increase of the temperature, the polymer chains are in solution, as shown in Figure 3. 9 (b).

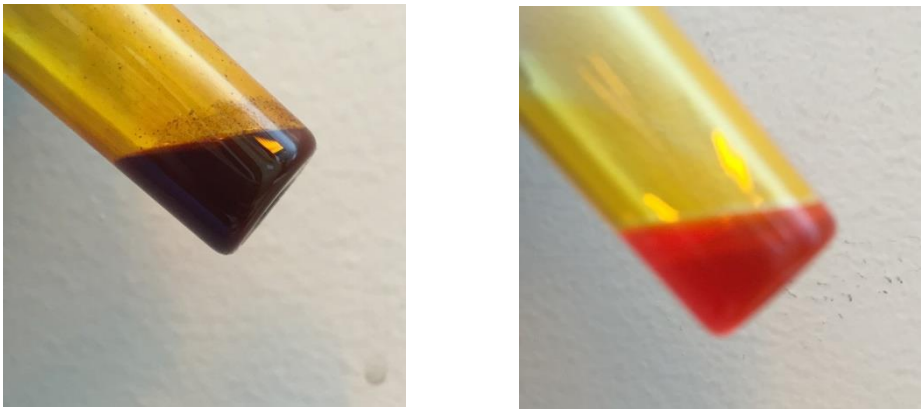

(a) (b)

Figure 3. 9 Photographic image of poly(3-hexylthiophene) (P3HT) with 23,000 g/mol molecular weight in Toluene of 1 wt. % at (a) room temperature; and (b) elevated temperature, respectively.

Figure 3. 10 shows the TG/DTA curve of P3HT-b-PTMA. From the thermogravimetric curve (the blue solid line), we could calculate the decomposition temperature (T_d) at around 220 ℃, as well as the glass transition temperature (T_g) which is around 180 ℃. From the differential thermal analysis curve (the red solid line) we could see that there are no obvious endothermic or exothermic peaks, which indicates that during the whole elevation of temperature from 25 ℃ to 600 ℃, the microstructure has not become more ordered or disordered. In other words, the microstructure of the diblock copolymer powders might have already been crystalized after they are purified and gathered together and before the thermal analysis.

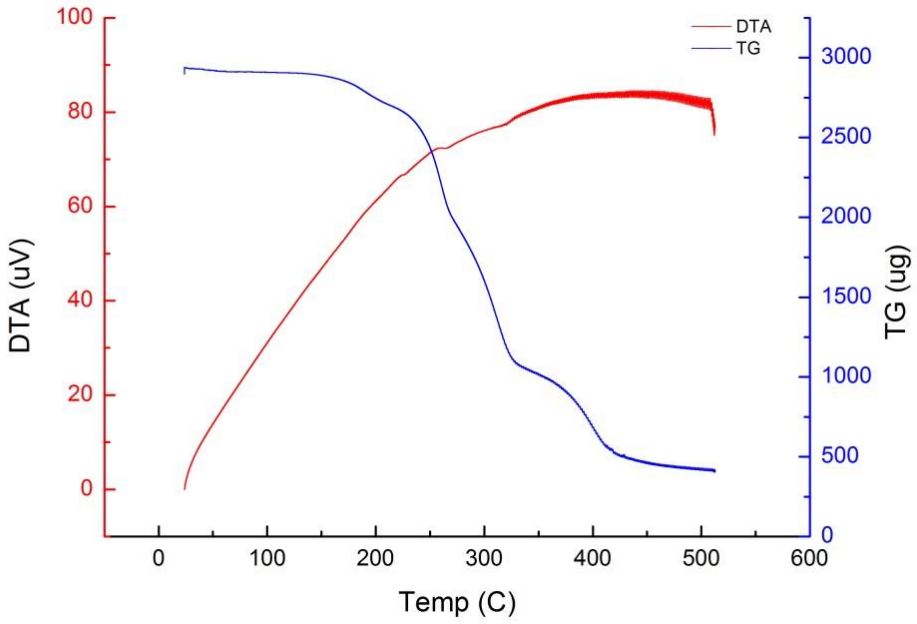

Figure 3. 10 TG/DTA curve of poly(3-hexylthiophene)-*b*-poly(2,2,6,6-tetramethyl-4-piperidinyloxymethacrylate) (P3HT-*b*-PTMA) powders, elevated from 25 ℃ to 600 ℃, at a scan rate of 10 ℃ /min, and held at 600 ℃ for 5 min. .

Since the diblock copolymer will not become more ordered at elevated temperature, during the AFM sample preparations, we did not conduct thermal annealing although it is a common annealing method for the majority of AFM sample preparation. For all the other AFM sample preparations, two coating methods were applied, which include spin-coating and drop-casting. The homopolymer of P3HT and the diblock copolymer P3HT-*b*-PTMA are dissolved in tetrahydrofuran, chloroform, benzene, toluene, and/or chlorobenzene, and then annealed for 24 hours under the same solvent.

Figure 3. 11 shows the AFM phase images of homopolymer P3HT with different molecular weights. Both samples are dissolved in toluene, then spin-coated onto the pre-cleaned glass substrate, and finally annealed under toluene for 24 hours. The one with lower

molecular weight of 11,000 g/mol forms better aligned nanofibrils, as shown in Figure 3. 11 (a). This indicates that the nanofibrils are composed of extended chains, with the backbone being in the plane of the film. In contrast, the one with higher molecular weight of 23,000 g/mol forms interconnected but less-ordered nanofibrils, as shown in Figure 3. 11 (b). This is because the relatively high stiffness of the conjugated backbone may induce stress on the stacking of the chains during chain folding, which leads to decreasing order and thus less-defined nanostructures. This result indicates that the P3HT has very strong π-π stacking interaction which makes it easy for chains to interconnect, and thus a large molecular weight of P3HT will lead to less or even lack of order.

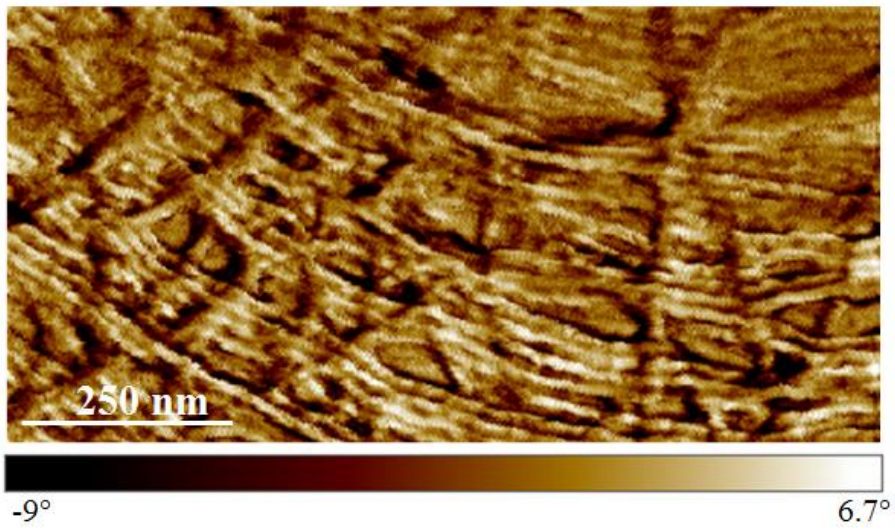

(a)

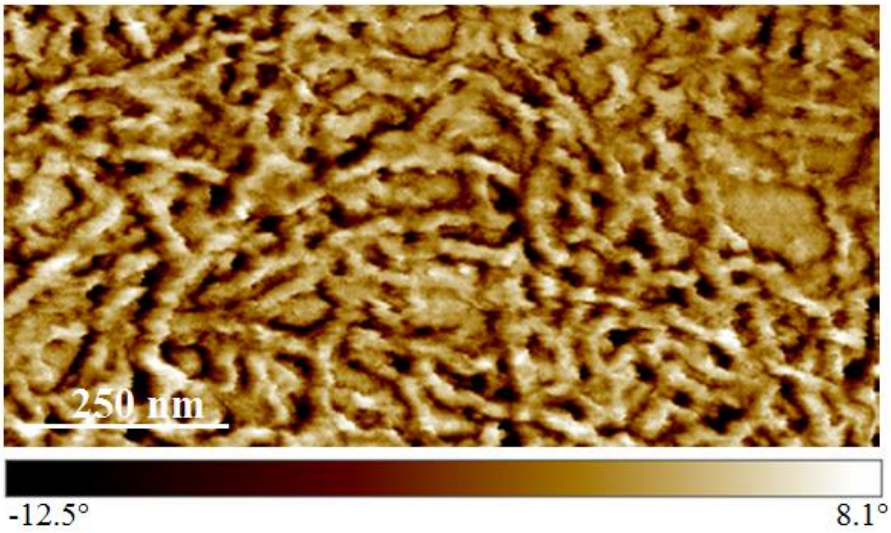

(b)

Figure 3. 11 AFM phase images of homopolymer P3HT films spin-coated from toluene solution, and solvent annealing with toluene for 24 hours, of different molecular weights (a) 11,000 g/mol; and (b) 23,000 g/mol.

Figure 3. 12 shows the AFM phase images of P3HT(11K)-*b*-PTMA(18K) diblock copolymer in different solvents using different coating methods. Block copolymer in Figure 3. 12 (a) is dissolved in chloroform by spin-coating, and then annealed in chloroform for 24 hours. The small white circles encompass pink and dark brown spots, which indicate the noise and/or topology artifacts. The large white circle contains tiny stripe-like figures, but the separation distance is shorter than that in Figure 3. 11 AFM phase images of homopolymer P3HT films spin-coated from toluene solution, and solvent annealing with toluene for 24 hours, of different molecular weights (a) 11,000 g/mol; and (b) 23,000 g/mol. Figure 3. 12 (b) has similar phase image as (a) does. Block copolymers in Figure 3. 12 (c) are dissolved in chlorobenzene by drop-casting, and then annealed in chlorobenzene for 24 hours. The overall image contains hole-like structures which is different with (a) and (b).

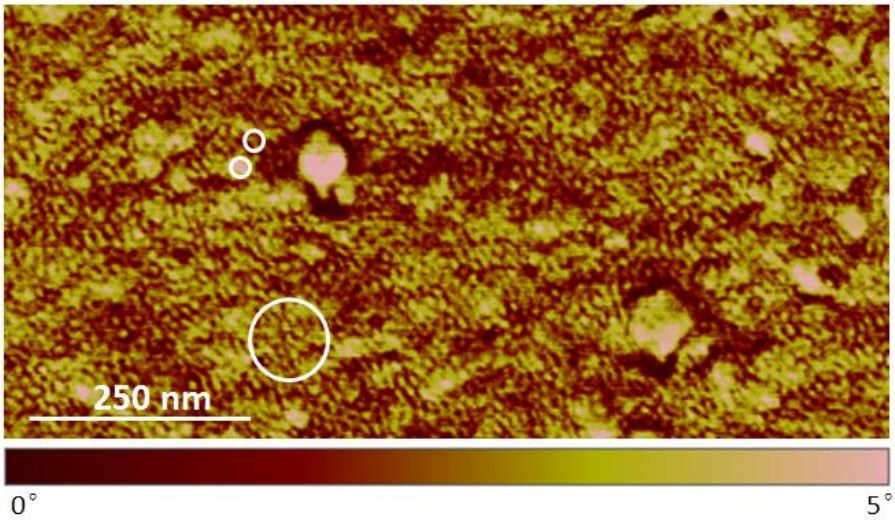

(a)

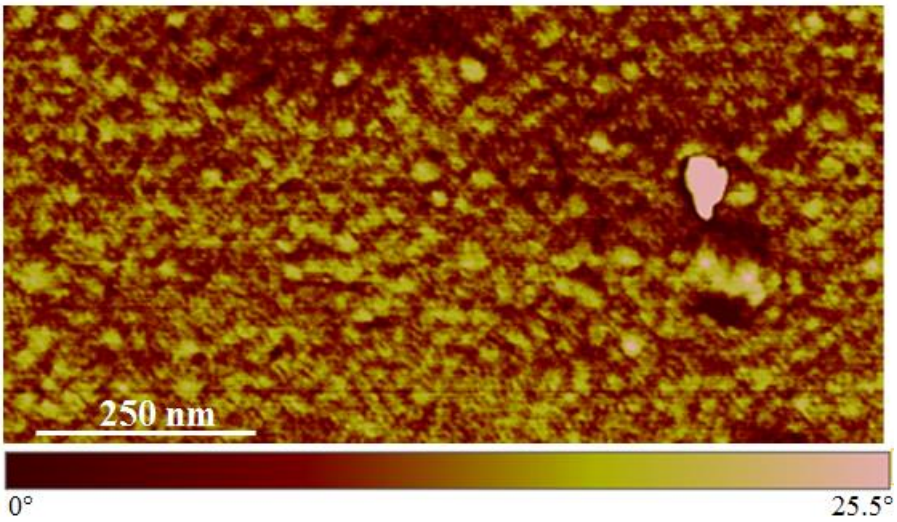

(b)

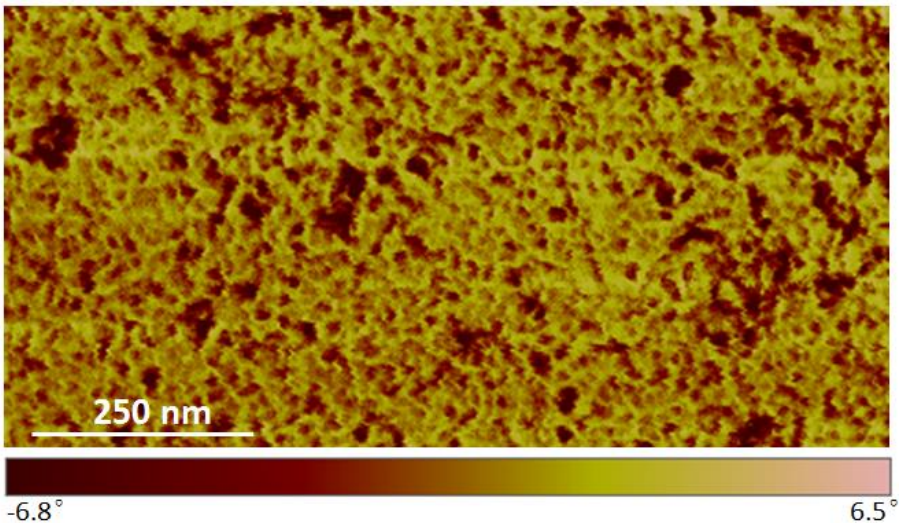

(c)

Figure 3. 12 AFM phase images of P3HT(11K)-b-PTMA(18K) diblock copolymer in (a) chloroform through spin-coating, and then annealed with chloroform for 24 hours; (b) THF through spin-coating, and then annealed with THF for 24 hours ; (c) chlorobenzene through drop-casting, and then annealed with chlorobenzene for 24 hours.

3.4 Electrical characterization results

3.4.1. Resistance

Many resistors and conductors have a uniform cross section with a uniform flow of electric current, and are made of one material, as shown in Figure 3. 13.

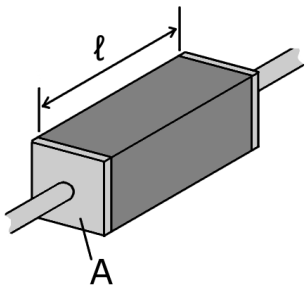

Figure 3. 13 Scheme of a piece of resistive material with electrical contacts on both ends.

The resistance of an electrical conductor is a measure of the difficulty to pass an electric current through that conductor. In this case, the electrical resistance R is defined by Pouillet's law, which given by $A = a \times b$ Equation 3. 1.

$$R = \rho \frac{l}{A}$$

$$A = a \times b \qquad \text{Equation 3. 1}$$

where R is the electrical resistance of a uniform specimen of the material (measured in ohms, Ω); l is the length of the piece of material (measured in metres, m); A is the cross-sectional area of the specimen (measured in square metres, m^2), and is defined by the product of a, the height of the cross-section, and b, the length of the cross-section; ρ is the electrical resistivity, which is every material's intrinsic and characteristic property (measured in ohm-meters, Ω • m). From Pouillet's law we see the resistance of a given material increases with length, but decreases with increasing cross-sectional area.

Figure 3. 14 shows the scheme of the resistance measurement device. This device is made by two 2 mm lengths of gold wires with a separation distance of 2 μm, on a pretreated silica substrate. After spin-coating the P3HT homopolymer or P3HT-*b*-PTMA diblock copolymer onto the device chip, shown by the violet area, an external voltage is applied to measure the polymer resistance. And then the film thickness is measured to support the results.

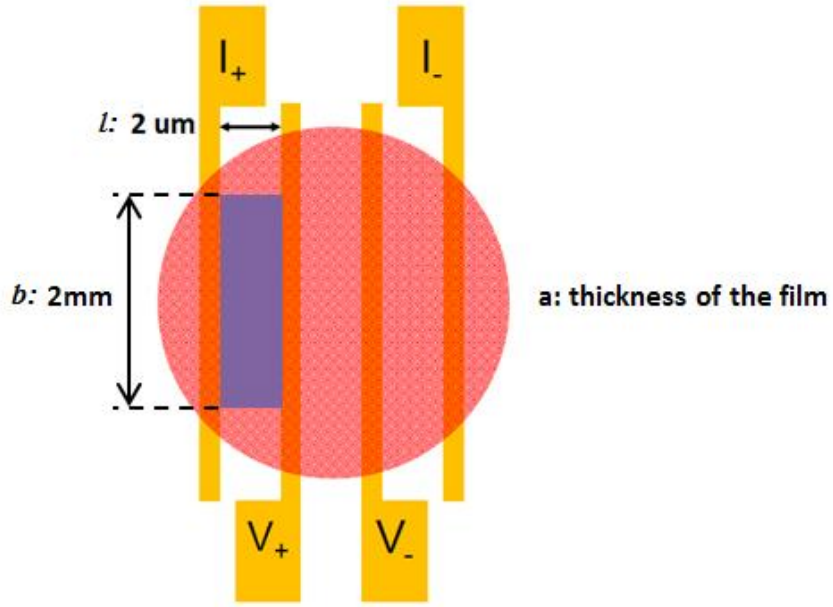

Figure 3. 14 Top view of the scheme of the resistance measurement device. Yellow lines indicate gold wires; violet area indicates the coated polymer film.

Table 3. 5 summarizes the resistance and film thickness of P3HT homopolymer with molecular weight of 11,000 g/mol. From the table, the film thickness does not correspond well with the resistance through Pouillet's law. This might because the magnitude of the film thickness is comparable to that of the length of the polymer film. In detail, since the electrons transport through the shortest way, if the film thickness is too large as compared to the length, the thicker part of the film will not become a part of the transportation way, and thus this part is useless.

Table 3. 5 Summary of the resistance and film thickness of P3HT (11K) homopolymer.

P3HT	1	2
Resistance (Ohm)	142K	8.67M
Film thickness (um)	0.590	2.700

However, the conductivity of the P3HT-*b*-PTMA block copolymer cannot be measured. It appears that in the undoped block copolymer the resistance of both phases of the diblock copolymer are insulating. These measurments and others made on additional polymers in the group are consistent with recent results of several groups but are in contradiction to several measurements reported in the literature. The fact that the undoped blocks are insulating is a strong indicator that the polymers made in this study are pure and once doped will provide for some interesting conductivity measurements.

In preparation for these measurements, we have designed several architectures for the device. The first design is shown in Figure 3. 15, which is sandwich-like and gives the side view of the design of the device. The top gold layer is the gold plate; the violet layer in between is the polymer thin film; the followed pink layer is the substrate. The advantage of this mode is that, the A in Pouillet's law is magnificently enlarged, while the length in Pouillet's law is comparably sharply shortened.

Figure 3. 15 Side view of the sandwich-like design of the device.

The second design is shown in Figure 3. 16, which is comb-like and gives the top view of the design of the device. The gold combs are gold wires; the violet areas in between are the coated polymer thin film; the pink area is the substrate. The characteristic of this device is that every two gold electrodes and the violet polymer film in between forms a resistor. Every resistor is connected parallel in parallel. To find the total resistance of all components, the reciprocals of the resistances R_i of each component are summed and the reciprocal of the sum is calculated. Total resistance will always be less than the value of the smallest resistance. The formula to find the total resistance is expressed by $R_{total} = \frac{R}{N}$. Therefore, the advantage of this device is that, with each increase in the number of electrodes, accuracy is improved.

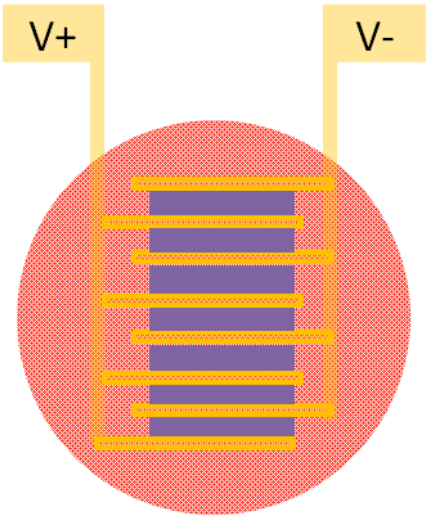

Figure 3. 16 Top view of the comb-like design of the device.

The third design is shown in Figure 3. 17, which is spiral and gives the top view of the design of the device. The green and red lines are the two gold wire connected to positive and negative voltage, respectively. The violet areas in between are the coated polymer thin film. The pink area underneath is the substrate. The advantage of this device is that the spiral lines could be as tight as needed, and thus the A in Pouillet's law is enlarged as needed, while the length in Pouillet's law remains the same.

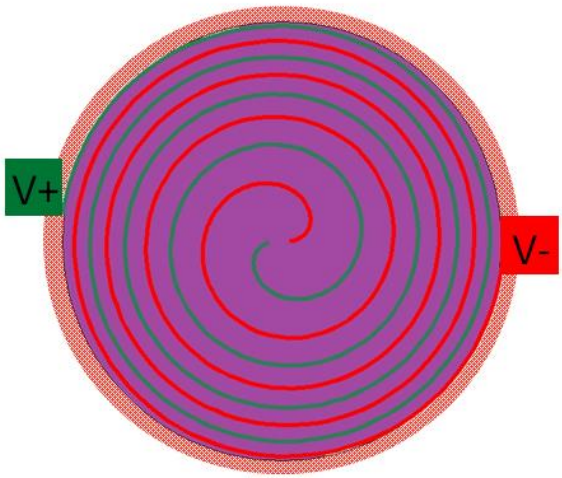

Figure 3. 17 Top view of the spiral-like design of the device.

3.4.2. Electron Spin Resonance (ESR)

Electron spin resonance (ESR) or electron paramagnetic resonance (EPR) spectroscopy is a method for studying materials with unpaired electrons. The basic concepts of EPR are analogous to those of nuclear magnetic resonance (NMR), but it is electron spins that are excited instead of the spins of atomic nuclei. EPR spectroscopy is particularly useful for studying metal complexes or organic radicals.

Figure 3. 18 shows the ESR spectra of TEMPO standard (a) and P3HT-*b*-PTMA diblock copolymer (b). The nitroxide polymers are paramagnetic because of the NO radicals.

Therefore, ESR spectroscopy can be used to determine the fraction of oxidation of the amine to the NO radical. We use the integration of the ESR spectrum of TEMPO standard as reference for 100 % stable radical groups. In other words, every repeat unit has one pendent stable radical (TEMPO) on it. Therefore, under the situation that all the samples are made at the same known spin concentration, it is possible to obtain of the conversion of the stable radical groups by integration from the ESR spectrum of a test diblock copolymer.

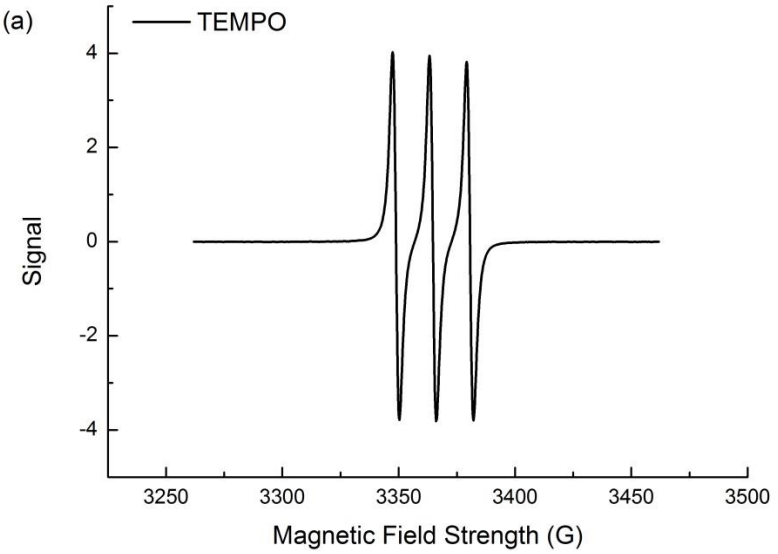

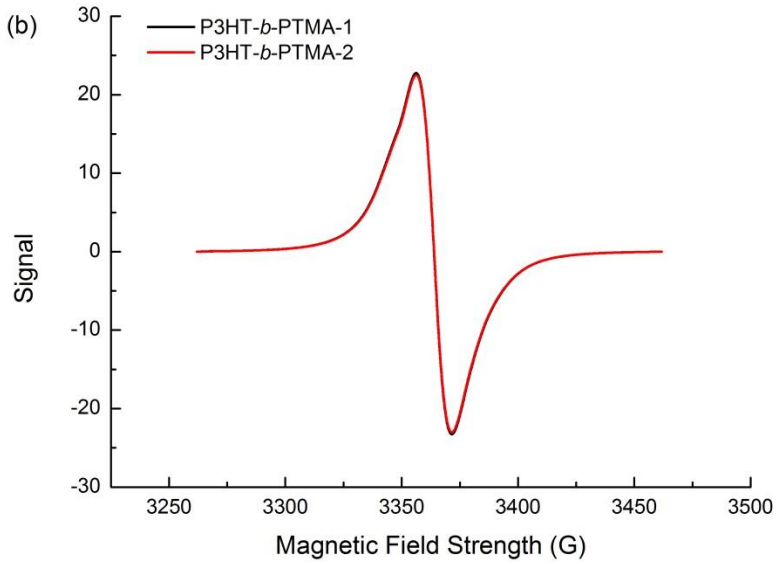

Figure 3. 18 ESR spectra of (a) TEMPO as standard; and (b) P3HT-*b*-PTMA diblock copolymer.

Chapter 4 Discussions of block copolymer characterization

4.1 Introduction

In this chapter, we compare and discuss with the physical characterization of the newly synthesized stable radical containing polymers with respect to published work together with the microstructure and electrical properties of our P3HT homopolymers and P3HT-*b*-PTMA diblock copolymers, which were already mentioned in chapter 3. While we were inspired to study the fundamental mechanisms of energy storage according to P3HT-*b*-PTMA, there exist many rod-coil block copolymers, conjugated-non conjugated polymers, conjugated-stable radical polymers under investigation, which resemble our prototype materials. We discuss the molecular characteristics of P3HT revealed by π-π interactions in UV-vis spectroscopy and AFM phase images, as well as how to optimize the conditions in the synthesis process. Also, we discuss other research methods as a the means of improving diblock copolymer phase separation and how it can be measured through AFM. Finally we analyze the electrical properties of homopolymers and block copolymers synthesized through other workers and compare them to our studies.

4.2 Block copolymer compositions

Poly(3-hexylthiophene) has high conductivity and good solubility due to its conjugated structure and its flexible side chains, respectively. However, due to its semi-rigid structure, the mechanical and processing properties of the P3HT are complex. In order to enhance its properties processing and performance, the several groups have integrated P3HT in copolymer structures with various flexible polymer chains, such as polystyrene (PS) or poly(methyl acrylate) (PMA), so that the desired mechanical properties may be achieved

[70][71]. In order to take advantage of and maintain the high electrical conductivity of P3HT in rod-coil block copolymers, Fréchet et al. linked the conjugated P3HT with C_{61}-butyric acid methyl ester (PCBM) or poly(acrylic acid) (PAA) [72][73].

Poly(2,2,6,6-tetramethylpiperidinyloxy methacrylate) (PTMA) as an electronically active polymer has been widely investigated for applications for its superior charge-transfer and charge-storage properties. While the Nakahara and Nishide groups firstly reported applying PTMA to organic rechargeable devices as a new cathode material [74], the Suga group demonstrated for the first time the formation of thin-film structures in radical containing diblock systems. However, their results did not show well-ordered behavior or long-range order [75]. Subseqently, several research groups have synthesized and assembled the PTMA-containing diblock copolymers to investigate their microstructures, with structures such as PTMA-*b*-PS and PTMA-*b*-PDMS. [76][77].

One major challenge for PTMA lies in the insulating nature of the polymer backbone. The electronic conductivity of nitroxide radical-based polymers is in the range of 10^{-6} S•cm^{-1}[78]. To accommodate the polymer's low electronic conductivity, PTMA electrodes are blended with excess amounts of carbon black additives. However, this in return reduces the electrode capacity [79]. In order to solve this issue, to design an intrinsically conductive block copolymer with organic radical pendent groups by means of a conjugated backbone is a reasonable method. In recent years, Masuda et al. incorporated polyacetylenes into TEMPO-containing blocks [80]. Zhang et al. synthesized PTMA block polypyrrole derivatives (PTMA-*b*-PPy) as cathode materials [81]. Beside chemical synthesis, Lutkenhaus et al. conducted electro-polymerization to synthesize P3HT carrying pendent TEMPO groups directly substituted onto the side chain which is linked by ether groups [82].

Although great attention has been paid to the application of PTMA and P3HT related battery materials, there is little focus on the fundamental mechanisms about the unpaired electron radical transport. Therefore, our inspiration is to design the block copolymer which takes advantages of the high conductivity and good solubility of P3HT together with stable radical polymer PTMA to investigate conduction mechanisms.

According to literature reports, ATRP of the TMPM monomer would be inefficient because the monomer contains a secondary amine, which would interfere with chelation of the catalyst [83]. In order to improve the synthetic procedure, the Lee group has studied the conditions for ATRP and optimized them by examination of a series of model polymerizations using small molecule initiator [84]. They concluded that the HMTETA ligand is better in ATRP, and the optimal ratio of CuBr to the HMTETA ligand is 1:3, and the optimal molar ratio of catalyst to initiator is 1:1. In our research, mentioned in 2.4 Exemplary synthesis routes, the ratio [P3HT-initiator]:[CuBr]:[HMTETA]= 1:1:3 was used. This minor adjustment was applied based on our polymerization using macro-initiator, while their optimal parameters were obtained from polymerization of ethyl bromo isobutyrate initiator.

According to the diblock copolymer composition and structure, McCullough et al. have synthesized P3HT-*b*-PMA, which resembles our P3HT-*b*-PTMA [64]. The results obtained are shown in Table 4. 1.

Table 4. 1 Composition of poly(3-hexylthiophene)-b-poly(methyl acrylate) diblock copolymers [64]

	PHT (mol%)	PMA (mol%)	M_n (GPC)	PDI (GPC)
1	100	0	12200	1.17
2	97.0	3.0	12290	1.24
3	67.0	33.0	14350	1.27
4	52.4	47.6	15180	1.33
5	42.5	57.5	15340	1.49
6	41.2	58.8	15400	1.6

Compared with our results mentioned in Table 3. 4, we could see that both molecular weights obtained by GPC are increasing with the increase of the addition of the second block by ATRP. However, the dispersities increase as a trade-off to higher PMA molecular weights.

4.3 Block copolymer micro-structure discussions

The rigidity and planar conformation of the conjugated backbone of P3HT allows efficient packing and crystallization. In the meantime, aggregation is driven by strong π-π interactions perpendicular to the conjugated backbone, as well as by hydrophobic interactions of the side chains. Adachi et al. [85] have plotted similar UV-vis absorbance-wavelength graphs of different molecular weights of P3HT as we mentioned about data shown in Figure 3. 8. As reported by Samitsu et al. [86], an obvious color change of P3HT in anisole from 60 ^{o}C to room temperature was observed, which was demonstrated in our results before in Figure 3. 9. Furthermore, Guillerez et al. [87] reported that there would be an evolution of the solution spectrum from 80 ^{o}C cooling to room temperature, from a single and broad absorption peak to

one large peak together with two minor peaks, which indicated aggregate formation in solution during the cooling process. Figure 4. 1 shows the relevant results.

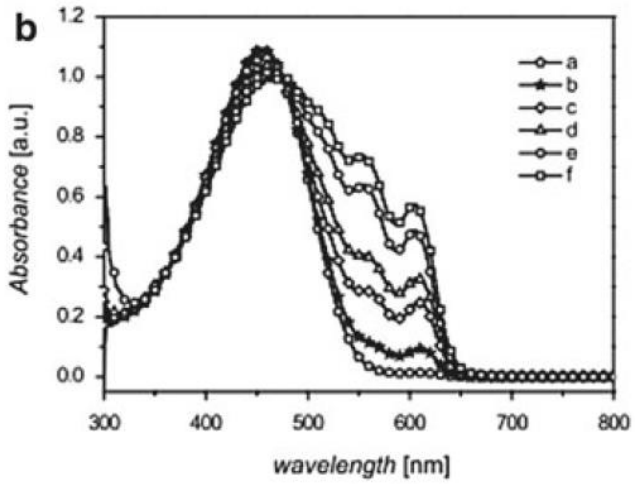

Figure 4. 1 Absorption spectra of P3HT in *p*-xylene (1 wt%) after dissolution at 80 ^{o}C and subsequent cooling to room temperature at 20 ^{o}C/h. Evolution of the solution was followed at room temperature, with the spectra being taken after (a)2 h, (b)4 h, (c)6 h, (d)21 h, (e)28 h, and (f)48 h [87].

The thin-film self-assembly behavior of block copolymers containing both relatively flexible (coil-like) segments and rigid (rod-like) segments has been investigated widely from theoretical, computational, and experimental prospective by the Ganesan et al. [88][89]. The introduction of semiconducting moieties (rod segment) in block polymer materials has been increasingly studied. However, the existence of π-conjugated moieties usually results in more complicated microphase separation behavior, which leads to block polymer systems rarely self-assembling into the more often-observed coil-coil nanostructures, such as hexagonally packed cylinders and gyroid structures [90].

The Baek group focused phase morphology of different molecular weights of P3HT, as well as the phase separation of poly(3-hexyl thiophene)-block-poly(methyl methacrylate) (P3HT-*b*-PMMA) for various film thicknesses [91]. For P3HT, they concluded the film morphology depended significantly on molecular architecture, and indicated that the P3HT

nanofibrils were elongated by π-π stacking between extended backbones. For P3HT-*b*-PMMA, they proposed a critical thickness, below which the film surface morphology was a hexagonal array of vertical P3HT nanodomains, and above which the morphology was covered with laterally assembled nanofibrils. This is shown in Figure 4. 2. We have demonstrated our results in Figure 3. 11 and Figure 3. 12, which have the same tendency but are relatively crude and rough. This may be due to the the fact that spin-coating and solvent annealing techniques have not been optimized.

Beside changing the film thickness to improve phase separation, Jo et al. tried blending films of P3HT-b-PMMA with PMMA to achieve optimized microstructure [92]. Reichmanis et al. studied the solvent based hydrogen bonding factor to impact polymer nanoscale morphology [93].

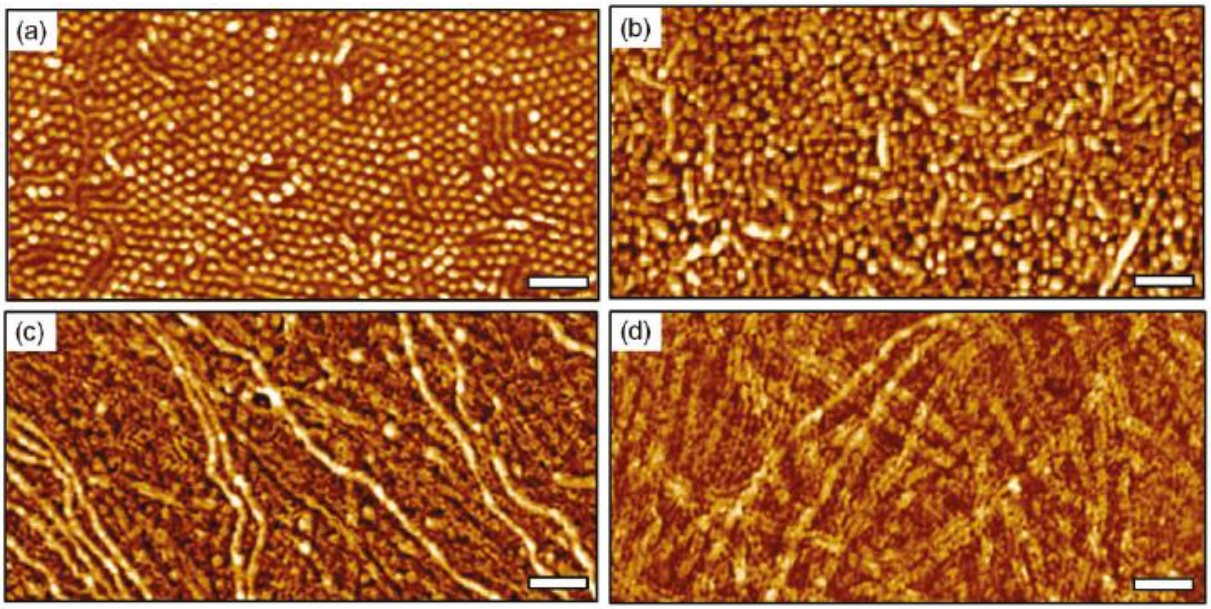

Figure 4. 2 AFM phase images of P3HT-b-PMMA films with various thickness cast from CB onto the SiO2/Si substrates: (a)20nm; (b)30nm; (c)50nm; (d)80nm [91].

4.4 Block copolymer electrical properties

Recently, several groups have reported various types of π-conjugated diblock copolymers with high conductivity. Su et al. reported well-defined conducting domains with poly(3-hexylthiophene)-block-poly(2-vinylpyridine) (P3HT-*b*-P2VP) in bulk [94]. McCullough et al. reported conductivity (σ) of 4 S/cm for P3HT-*b*-PMA with 58% molar ratio of PMA in the block copolymer [64]. Kowalewski and coworkers reported that the conductivity of P3HT precursor is higher than that of the diblock copolymers [95]. The relatively high conductivities were only observed for diblock copolymers of P3HT-*b*-PMMA and P3HT-*b*-poly(*t*-BuMA) when the polymers had nanofibrillar morphologies with densely packed nanofibrils.

The Lee group [84] has studied the ESR spectra of 2,5-poly(3-[1-ethyl-2-(2-bromoisobutyrate)]thiophene)-graft-poly(2,2,6,6-tetramethylpiperidin-1-oxyl-4-yl methacrylate) (PEBBT-*g*-PTMA), PTMA and PEBBT. The oxidation yield of PEBBT-*g*-PTMA and PTMA is 56% and 80%, respectively. Similar to our results mentioned in Figure 3. 18, the oxidation yield of block copolymer is less than that of PTMA homopolymer, which may be due to the steric effect of the chains. Figure 4. 3 shows their ESR results.

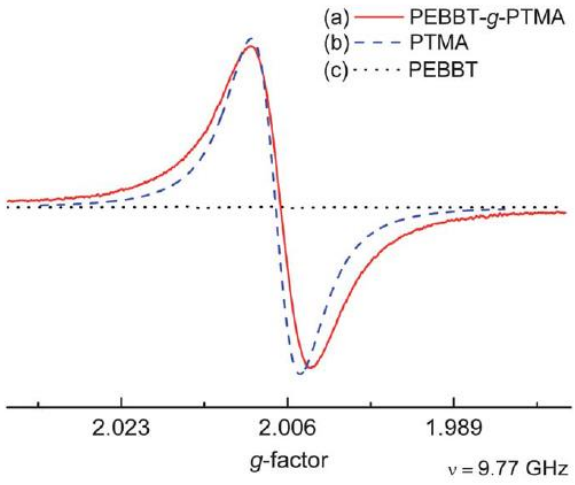

Figure 4. 3 EPR spectra of (a) PEBBT-g-PTMA, (b) PTMA, and (c) PEBBT [84].

References

[1] Darling S B. Directing the self-assembly of block copolymers[J]. Progress in Polymer Science, 2007, 32(10): 1152-1204.
[2] Friend RH, Gymer RW, Holmes AB, Burroughes JH, Marks RN, et al. 1999.Nature 397:121–28
[3] Oyaizu, K.; Nishide, H. Adv. Mater. 2009, 21, 2339–2344.
[4] Murata, H.; Miyajima, D.; Nishide, H. Macromolecules 2006, 39, 6331–6335.
[5] Pu, Y.-J.; Soma, M.; Kido, J.; Nishide, H. Chem. Mater. 2001, 13, 3817–3819.
[6] Chiang, C. K.; Park, Y. W.; Heeger, A. J.; Shirakawa, H.; Louis, E. J.; MacDiarmid, A. G. Phys. Rev. Lett. 1977, 39, 1098.
[7] See, for instance: Handbook of Conducting Polymers, 2nd ed.; Skotheim, T. A., Reynolds, J. R., Elsenbaumer, R. L., Eds.; Marcel Dekker: New York, 1997.
[8] Tang, C. W.; VanSlyke, S. A. Appl. Phys. Lett. 1987, 51, 913.
[9] Brédas J L, Beljonne D, Coropceanu V, et al. Charge-transfer and energy-transfer processes in π-conjugated oligomers and polymers: a molecular picture[J]. Chemical Reviews, 2004, 104(11): 4971-5004.
[10] Tourillon G, Garnier F (1983) Stability of conducting polythiophene and derivatives. J Electrochem Soc 130:2042–2044.
[11] Sirringhaus, H.; Tessler, N.; Friend, R. H. Science 1998, 280, 1741–1744.
[12] Sauvé, G.; McCullough R. D. Adv. Mater. 2007, 19, 1822–1825.
[13] Thompson, B. C.; Fréchet, J. M. J. Angew. Chem. Int. Ed. 2008, 47, 58–77.
[14] Woo, C. H.; Thompson, B. C.; Kim, B. J.; Toney, M. F.; Fréchet, J. M. J. J. Am. Chem. Soc. 2008, 130, 16324–16329.
[15] McCullough R D, Ewbank P C. Regioregular, head-to-tail coupled poly (3-alkylthiophene) and its derivatives[J]. Handbook of conducting polymers, 1998, 2: 225-258.
[16] Hicks R G. What's new in stable radical chemistry?[J]. Organic & biomolecular chemistry, 2007, 5(9): 1321-1338.
[17] N. Jux, K. Holczer and Y. Rubin, Angew. Chem., Int. Ed. Engl., 1996, 35, 1986–1990.
[18] B. T. King, B. C. Noll, A. J. McKinley and J.Michl, J. Am. Chem. Soc., 1996, 118, 10902–10903.
[19] M. M. Olmstead, L. H. Pu, R. S. Simons and P. P. Power, Chem. Commun., 1997, 1595–1596.
[20] R. A. Sheldon, I. Arends, G. J. Ten Brink and A. Dijksman, Acc. Chem. Res., 2002, 35, 774–781.
[21] J. S. Wright, D. J. Carpenter, D. J. McKay and K. U. Ingold, J. Am. Chem. Soc., 1997, 119, 4245–4252.
[22] J. C. Scaiano, A.Martin, G. P. A. Yap and K. U. Ingold, Org. Lett., 2000, 2, 899–901.
[23] W. Kaim, Coord. Chem. Rev., 1987, 76, 187–235.
[24] C. J. Hawker, A. W. Bosman and E. Harth, Chem. Rev., 2001, 101, 3661–3688.
[25] J. Stubbe and W. A. van der Donk, Chem. Rev., 1998, 98, 705–762.
[26] P. P. Power, Chem. Rev., 2003, 103, 789–809.
[27] T. Chivers, M. N. S. Rao and J. F. Richardson, J. Chem. Soc., Chem. Commun., 1983, 186–187.

[28] Likhtenshtein, G. I.; Yamaguchi, J.; Nakatsuji, S.; Smirnov, A. I.; Tamura, R. Nitroxides; Wiley-VCH: Weinheim, 2008.
[29] A. R. Forrester, J. M. Hay and R. H. Thomson, Organic Chemistry of Stable Free Radicals, Academic Press, London, 1968.
[30] Suga, T.; Pu, Y.-J.; Oyaizu, K.; Nishide, H. Bull. Chem. Soc. Jpn. 2004, 77, 2203–2204.
[31] Oyaizu K, Nishide H. Radical polymers for organic electronic devices: a radical departure from conjugated polymers? [J]. Advanced Materials, 2009, 21(22): 2339-2344.
[32] Ohta, T. and Kawasaki, K. (1986) Macromolecules 19, 2621-2632.
[33] Ates, F. S. and Fredrickson, G. H. (1990) Annual Reviews physical Chemistry 41, 525-557.
[34] Matsen, M. W. and Schick, M. (1994) Physical Review letters 72, 2660-2663.
[35] Bates, F. S. (1991) Science 251, 898-905.
[36] Sakurai, S., Momii, T., Taie, K., Shibayama, M., Nomura, S., and Hashimoto, T. (1993) Macromolecules 26, 485-491.
[37] Hong, K. M. and Noolandi, J. (1983) Macromolecules 16, 1093-1093.
[38] Hashimoto, T., Shibayama, M., and Kawai, H. (1983) Macromolecules 16, 1093-1101.
[39] Meyer V (1883) Thiophene, a substance contained in coal-tar benzene. Chem Ber 16:1465–1478.
[40] Meyer V (1884) The thiophene and pyrroline groups. Chem Ber 16:2968–2975.
[41] Meisel SL, Johnson GC, Hartough HD (1950) Polymerization of thiophene and alkylthiophenes. J Am Chem Soc 72:1910–1912.
[42] Armour M, Davies AG, Upadhyay J, Wassermann A (1967) Colored, electrically conducting polymers from furan, pyrrole, and thiophene. J Polym Sci A-1 Polym Chem 5:1527–1538.
[43] Ramsey JS, Kovacic P (1969) Polymerization of aromatic nuclei. XV. Polymerization of 2,5-di- and 2,3,5-trichlorothiophenes with aluminum chloride-cupric chloride. J Polym Sci A-1 Polym Chem 7:127–138.
[44] Curtis RF, Jones DM, Thomas WA (1971) The ‘trimer’ and ‘pentamer’ from the polymerization of thiophene by polyphosphoric acid. J Chem Soc C 1971:234–238.
[45] Tourillon G, Garnier F (1982) New electrochemically generated organic conducting polymers. J Electroanal Chem Interfacial Electrochem 135:173–178.
[46] Yamamoto T, Sanechika K, Yamamoto A (1980) Preparation of thermostable and electricconducting poly(2,5-thienylene). J Polym Sci Polym Lett Ed 18:9–12.
[47] Yamamoto T, Sanechika K, Yamamoto A (1983) Preparation and characterization of poly(thienylenes). Bull Chem Soc Jpn 56:1497–1502.
[48] Chen TA, Rieke RD (1992) The first regioregular head-to-tail poly(3-hexylthiophene-2,5-diyl) and a regiorandom isopolymer: nickel versus palladium catalysis of 2(5)-bromo-5(2)-(bromozincio)-3-hexylthiophene polymerization. J Am Chem Soc 114:10087–10088.
[49] McCullough RD, Lowe RD (1992) Enhanced electrical conductivity in regioselectively synthesized poly(3-alkylthiophenes). J Chem Soc Chem Commun 1992(1):70–72.
[50] Loewe RS, Khersonsky SM, McCullough RD (1999) A simple method to prepare head-to-tail coupled, regioregular poly(3-alkylthiophenes) using Grignard metathesis. Adv Mater 11:250.

[51] Tamao K, Sumitani K, Kumada M (1972) Selective carbon–carbon bond formation by crosscoupling of Grignard reagents with organic halides. Catalysis by nickel-phosphine complexes. J Amer Chem Soc 94:4374–4376.
[52] Yamamoto T, Wakabayashi S, Osakada K (1992) Mechanism of carbon-carbon coupling reactions of aromatic halides, promoted by Ni(COD)2 in the presence of 2,20-bipyridine and triphenylphosphine, to give biaryls. J Organomet Chem 428:223–237.
[53] Sheina EE, Liu J, Iovu MC, Laird DW, McCullough RD (2004) Chain growth mechanism for regioregular nickel-initiated cross-coupling polymerizations. Macromolecules 37:3526–3528.
[54] Iovu MC, Sheina EE, Gil RR, McCullough RD (2005) Experimental evidence for the quasi-"living" nature of the grignard metathesis method for the synthesis of regioregular poly (3-alkylthiophenes). Macromolecules 38:8649–8656.
[55] Szwarc, M. Nature 1956, 178, 1168.
[56] Matyjaszewski, K.; Gaynor, S. G. In Applied Polymer Science; Craver, C. D., Carraher, C. E., Jr., Eds.; Pergamon Press: Oxford, UK, 2000; p 929.
[57] Controlled Radical Polymerization; Matyjaszewski, K., Ed.; American Chemical Society: Washington, DC, 1998; Vol. 685.
[58] Matyjaszewski K, Xia J. Atom transfer radical polymerization[J]. Chemical reviews, 2001, 101(9): 2921-2990.
[59] Kato, M.; Kamigaito, M.; Sawamoto, M.; Higashimura, T.
[60] Matyjaszewski, K.; Wang, J. S. WO Pat. 9630421, U.S. Pat. 5,- 763,548.
[61] Matyjaszewski, K.; Coca, S.; Gaynor, S. G.; Nakagawa, Y.; Jo, S. M. WO Pat. 9801480, U.S. Pat. 5,789,487.
[62] Matyjaszewski, K.; Davis, K.; Patten, T.; Wei, M. Tetrahedron 1997, 53, 15321.
[63] Matyjaszewski, K. ACS Symp. Ser. 2000, 768, 2.
[64] Iovu M C, Jeffries-El M, Sheina E E, et al. Regioregular poly (3-alkylthiophene) conducting block copolymers[J]. Polymer, 2005, 46(19): 8582-8586.
[65] L. Rostro, A.G. Baradwaj, and B.W. Boudouris: Controlled radical polymerization and quantification of solid state electrical conductivities of macromolecules bearing pendant stable radical groups. ACS Appl. Mater. Interfaces 5, 9896 (2013).
[66] Iovu MC, Sheina EE, Sauve´ G, Jeffries-EL M, Cooper J, McCullough RD. Polym Prepr 2004;45(1):278.
[67] Holdcroft S (1991) Determination of molecular weights and Mark–Houwink constants for soluble electronically conducting polymers. J Polym Sci B Polym Phys 29:1585–1588.
[68] Miyakoshi R, Yokoyama A, Yokozawa T. Synthesis of Poly (3‐hexylthiophene) with a Narrower Polydispersity[J]. Macromolecular rapid communications, 2004, 25(19): 1663-1666.
[69] T.Yamamoto,Y. Murakami, M. Abla, Chem. Lett. 1999, 419.
[70] Liu J, Sheina E, Kowalewski T, McCullough RD. Angew Chem 2002; 41:329.
[71] M. Ng, L. Yu, Angew. Chem., Int. Ed. 2002, 41, 3598.
[72] K. Sivula, Z. T. Ball, N. Watanabe, J. M. J. Fre´chet, Adv.Mater. 2006, 18, 206.
[73] Craley C, Zhang R, Kowalewski T, et al. Regioregular Poly (3‐hexylthiophene) in a Novel Conducting Amphiphilic Block Copolymer[J]. Macromolecular Rapid Communications, 2009, 30(1): 11-16.

[74] Nakahara K, Iwasa S, Satoh M, et al. Rechargeable batteries with organic radical cathodes[J]. Chemical Physics Letters, 2002, 359(5): 351-354.
[75] T. Suga, M. Sakata, K. Aoki, and H. Nishide: Synthesis of pendant radicaland ion-containing block copolymers via ring-opening metathesis polymerization for organic resistive memory. ACS Macro Lett. 3, 703 (2014).
[76] G. Hauffman, J. Rolland, J.-P. Bourgeois, A. Vlad, and J.-F. Gohy: Synthesis of nitroxide-containing block copolymers for the formation of organic cathodes. J. Polym. Sci. Pol. Chem. 51, 101 (2013).
[77] Rostro L, Baradwaj A G, Muller A R, et al. Synthesis and thin-film self-assembly of radical-containing diblock copolymers[J]. MRS Communications, 2015, 5(02): 257-263.
[78] Rostro, L.; Baradwaj, A. G.; Boudouris, B. W. ACS Appl. Mater. Interfaces 2013, 5, 9896−9901.
[79] Kim, J.-K.; Cheruvally, G.; Ahn, J.-H.; Seo, Y.-G.; Choi, D. S.; Lee, S.-H.; Song, C. E. J. Ind. Eng. Chem. 2008, 14, 371−376.
[80] Qu, J.; Katsumata, T.; Satoh, M.; Wada, J.; Igarashi, J.; Mizoguchi, K.; Masuda, T. Chem. - Eur. J. 2007, 13, 7965−7973.
[81] Xu, L.; Yang, F.; Su, C.; Ji, L.; Zhang, C. Electrochim. Acta 2014, 130, 148−155.
[82] Li F, Zhang Y, Kwon S R, et al. Electropolymerized Polythiophenes Bearing Pendant Nitroxide Radicals[J]. ACS Macro Letters, 2016, 5(3): 337-341.
[83] J. Xia, X. Zhang and K. Matyjaszewski, Macromolecules, 1999, 32, 3531–3533.
[84] Lin C H, Chau C M, Lee J T. Synthesis and characterization of polythiophene grafted with a nitroxide radical polymer via atom transfer radical polymerization[J]. Polymer Chemistry, 2012, 3(6): 1467-1474.
[85] Zen A, Pflaum J, Hirschmann S, Zhuang W, Jaiser F, Asawapirom U, Rabe JP, Scherf U, Neher D (2004) Adv Funct Mater 14:757–764.
[86] Samitsu S, Shimomura T, Heike S, Hashizume T, Ito K (2008) Macromolecules 41:8000–8010.
[87] Berson S, De Bettignies R, Bailly S, Guillerez S (2007) Adv Funct Mater 17:1377–1384.
[88] B.D. Olsen, X. Li, J. Wang, and R.A. Segalman: Thin film structure of symmetric rod-coil block copolymers. Macromolecules 40, 3287 (2007).
[89] M. Shah and V. Ganesan: Correlations between morphologies and photovoltaic properties of rod-coil block copolymers. Macromolecules 43, 543.
[90] B.D. Olsen and R.A. Segalman: Self-assembly of rod–coil block copolymers. Mater. Sci. Eng. R 62, 37 (2008).
[91] Lee Y J, Kim S H, Yang H, et al. Vertical conducting nanodomains self-assembled from poly (3-hexyl thiophene)-based diblock copolymer thin films[J]. The Journal of Physical Chemistry C, 2011, 115(10): 4228-4234.
[92] Choi S Y, Lee J U, Lee J W, et al. Highly ordered poly (3-hexylthiophene) rod polymers via block copolymer self-assembly[J]. Macromolecules, 2011, 44(7): 1771-1774.
[93] Chang M, Choi D, Fu B, et al. Solvent based hydrogen bonding: impact on poly (3-hexylthiophene) nanoscale morphology and charge transport characteristics[J]. ACS nano, 2013, 7(6): 5402-5413.
[94] Dai, C. A.; Yen, W. C.; Lee, Y. H.; Ho, C. C.; Su, W. F. J. Am. Chem. Soc. 2007, 129, 11036.

[95] Iovu M C, Zhang R, Cooper J R, et al. Conducting Block Copolymers of Regioregular Poly (3‐hexylthiophene) and Poly (methacrylates): Electronic Materials with Variable Conductivities and Degrees of Interfibrillar Order[J]. Macromolecular Rapid Communications, 2007, 28(17): 1816-1824.